Contents lists available at ScienceDirect

Applied Catalysis B: Environmental

journal homepage: www.elsevier.com/locate/apcatb

Electrochemical CO_2 reduction coupled with alternative oxidation reactions: Electrocatalysts, electrolytes, and electrolyzers

Wanlong Xi [a,1], Peng Yang [a,1], Mingkun Jiang [a], Xiali Wang [a], Hexin Zhou [a], Junyuan Duan [a], Marina Ratova [b], Dan Wu [a,*]

[a] *Key Laboratory of Green Chemical Engineering Process of Ministry of Education, Hubei Key Laboratory of Plasma Chemistry and New Materials, School of Materials Science and Engineering, Wuhan Institute of Technology, Wuhan 430205, Hubei, PR China*
[b] *Faculty of Science and Engineering, Manchester Metropolitan University, Chester Street, Manchester M1 5GD, UK*

ARTICLE INFO

ABSTRACT

Electrocatalytic carbon dioxide reduction (CO_2RR) is a promising strategy to achieve carbon neutrality. Nevertheless, its practical viability is hindered by the energy-consuming anodic oxygen evolution (OER) process. In recent years, researchers have attempted to break this limitation by some novel anodic OER substitution reactions to improve the overall economic profitability. This article aims to provide a comprehensive review covering the recent development of integrated CO_2RR systems with alternative OER oxidation reactions. Starting from the presentation of fundamental considerations of electrolytic configurations, energy efficiency, value-added products and tech-economic analysis for high-performance integrations, the recent innovative anodic reactions are then summarized and thoroughly analyzed including the reactions involving alcohols, biomass, chlorine, water contaminants oxidations and chemicals electrosynthesis, with the focus on electrocatalysts design, electrolyte selection and system configurations. Finally, the current challenges and future perspectives are discussed to achieve the dual goals of sustainability and profitability in an economical and energy-efficient way.

1. Introduction

With the rapid development of industrialization and excessive uses of fossil fuels, the atmospheric CO_2 concentration has increased sharply [1–3]. By the end of the 21st century, the excessive amount of CO_2 in the atmosphere (the main component of greenhouse gases) is likely to increase global temperature by 2.3–5.4 ℃ [4], causing climate change and negatively impacting ecological balance. Moreover, the rapid depletion of nonrenewable fossil fuels will eventually lead to a worldwide energy crisis [5]. Hence, it is imperative to explore green energy sources and discover effective and efficient ways to converting CO_2 into high-value fuels and chemicals [6]. To this end, electrocatalytic reaction/technology powered by renewable energy (such as solar and wind energies) has emerged as a highly promising direction to converting CO_2 owing to its advantage of mild operation conditions [7]. In recent years, tremendous efforts have been devoted to converting CO_2 through CO_2RR to obtain value-added products, such as CO, CH_4, HCOOH, C_2H_4 and various hydrocarbons, all of which have wide industrial applications due to their

high energy densities [8]. For example, an expressive selectivity of higher than 90% at ampere-level industrial current densities has been achieved for the conversion of CO_2 to CO or HCOOH [9,10]. From an industrial application viewpoint, research efforts are to focus on high product yield with low energy input to make CO_2RR economically feasible for large scale production.

In conventional CO_2RR configurations, OER occurs at the anode to produce O_2 by water oxidization. Unfortunately, water oxidation is a four-electron transfer process with a large thermodynamic potential of 1.23 V [11], which accounts for more than 90% of the total system energy input [12]. In addition, anodically produced O_2 is usually released without any form of utilization due to its low value. Apart from the thermodynamics and kinetics concerns, reactive oxygen intermediates can also be produced during the OER process to shorten the life of the membrane inside the system [13]. So, a more thermodynamically friendly OER-alternative oxidation reaction is desirable to pair CO_2RR.

At present, many novel anodic reactions have appeared to assist

electrocatalytic CO_2 utilization. The first choice adopts the oxidation reactions with lower thermodynamic oxidation potentials than OER, which can reduce the electrolysis voltage and thus the total energy output of the reaction [14]. Enlightened from hybrid water electrolysis for energy-efficient H_2 production, thermodynamically favorable reactions such as alcohols, urea and hydrazine oxidations have been successfully employed to construct energy-saving CO_2RR integrated systems [15–17]. Researchers have noted that N_2 or CO_2 products being produced through complete oxidations are as low-value as O_2. Thus, numerous efforts have continued to look for anodic reactions suitable to CO_2RR for sustainability at both ends. On the one hand, specific substrates are chosen to be selectively oxidized to high-value products, making the whole system with higher economic benefits. Techno-economic analysis has highlighted significant economic feasibility of coupling CO_2RR with organics oxidation compared with CO_2RR||OER electrolysis [12]. At this point, selective oxidation of biomass or its derivations is considered as a feasible anode reaction. For example, the end-product 2,5-furandicarboxylic acid (FDCA), a platform chemical in biopolymer and pharmaceutical production, can be obtained from biomass-derived 5-hydroxymethylfurfural (HMF) [18]. On the other hand, some novel anodic reactions using wastewater contaminants as reactants have been reported to couple with CO_2RR from the perspective of simultaneous environmental remediation and CO_2 utilization [19]. Besides, seawater electrolysis realizes the coproduction of carbon-containing products from CO_2RR and Cl_2 from chlorine, enabling an energy-efficient way for valuable chemicals generation using natural resources and also providing starting materials for downstream reaction needs (such as phosgene synthesis). Inspiredly, pollutants removal through mineralization and important chemicals electrosynthesis through chemical oxidations have been successfully established to combine CO_2RR by taking the advantage of specific anodic reactions which generate highly oxidative species. Hence, integrating CO_2RR with these OER-alternative oxidation reactions opens a new door for value chain promotion at both ends through efficient use of energy inputs.

Building an integrated system is not a simple combination of cathode and anode, not to mention a long way from commercialization. High yields of valuable chemicals require properly designed electrode electrocatalysts with high selectivity, activity and endurance. At present, the exquisite design of the catalyst structures and components can achieve high catalytic performance, but in many cases the complicated preparation process involved is not conducive to large-scale industrial production in terms of technology feasibility and economic benefits. Moreover, the cathode and anode are also mutually influenced and restricted due to their different half-reaction operation conditions. As far as the electrolyte is concerned, CO_2RR is generally performed in $KHCO_3$ or KOH solution, while different types of anodic reactions are featured with different reactant solubility, catalyst characteristics and reactivity in acidic, neutral and alkaline solutions, making the choice of electrolyte more complicated. Although an ion exchange membrane (IEM) is employed to separate anode and cathode parts, membrane passivation and mass transfer between two sides also pose challenges to the electrocatalytic performance. Besides, the mismatch of the two sides will also add burdens to the cost of electrolyzer maintenance, product purification and collection. Moreover, the conventional CO_2RR||OER system has already achieved high selectivity (~100%) [20], high activity (>1 A cm^{-2}) [21] or high stability (>1000 h) [22] through the ingenious design of catalysts, electrodes and cell configurations. However, most of the current research on the integration systems is still in the early stage of exploring OER-alternative oxidation reactions to match CO_2RR using conventional H-type cells. Although high selectivity (~100%) to specific products can be achieved, the performance barriers of current density and catalyst durability are still unable to be broken. Referring to the high-performance CO_2RR||OER coupling system, it is expected to balance and design the indispensable components of electrodes, electrolytes and electrolyzers, ultimately accomplishing energy-saving and multifunctional coupling systems.

Recently, researchers have reviewed different types of pairing reactions with special emphasis on cell designs, organics conversion or electrochemical performance and economic viability [7,23,24]. In this review, we broadly cover recent endeavors for the integration of CO_2RR with OER-alternative anodic reactions regarding the important contributions of electrocatalysts, electrolytes and electrolyzers (Fig. 1). The major fundamental considerations for the integrated system in terms of electrolytic configurations, EE, value-added products and tech-economic analysis are presented. In the following sections, we will categorize the integrated systems into CO_2RR coupling with anodic oxidation alternatives including alcohols, biomass, chlorine, water contaminants oxidations reactions and chemicals electrosynthesis. Thereinto, the design principle of high-performance cathodic and anodic electrocatalysts towards specific value-added products and the corresponding reaction mechanism are emphasized. Moreover, the effect of catholyte and anolyte in terms of their compositions and reaction microenvironment, and electrolytic configurations including electrode assembly, membrane separator and electrolyzer construction determining the electrochemical performance are systematically discussed. Finally, the challenges facing the CO_2RR coupling integrated system based on the current studies, and opportunities regarding further accelerating the scientific research and industrial implantation are summarized.

2. Fundamental considerations for the integrated system

With respect to the integrated electrolysis system, the electrocatalysts, electrolytes, and electrolyzer configurations are indispensable components to perform redox reactions. Obviously, reasonable system design can ensure desirable products with satisfying practical and economic advantages. To better understand and evaluate the overall system, this section provides a basic introduction of fundamental considerations in terms of the electrolytic configuration, energy efficiency, value-added products, and tech-economic analysis.

2.1. The electrolytic configurations

Electrocatalysts and electrolytes are two prerequisites for cell configurations. Electrocatalysts as the most important factor affecting product performance can effectively produce specific products by reducing the reaction barrier and determining the reaction path [25]. Currently, the commonly used catalysts accommodable to the integrated system are mainly metal-based, carbon-based, and molecular catalysts functionalized with alloying, heteroatomic doping, defects, and other modification methods to further enhance catalytic performance [8]. Noteworthily, most of the presented research on catalysts concerning the system integration focus on the cathode side with more than 90% product selectivity. For example, by doping CuO with Sn atoms, the energy barrier for *COOH and *CO intermediates formation can be further reduced, finally achieving a 99.9% CO selectivity in the cathode with an overpotential of 420 mV [26]. To better enhance the overall performance of the integrated system, more focus should be placed to the rational design of anode catalysts. Furthermore, large-scale production of electrocatalysts in a green, cheap and sustainable manner towards commercialization is rarely achieved at present. Therefore, it is highly desirable to develop an eco-friendly and scalable technique to fabricate applicable anode and cathode catalysts to ensure technical feasibility.

Electrolytes as the conductive substrates determining the solubility of CO_2 as well as the pH of the cathode and anode have a strong impact on the electrochemical performance [27]. Among the most used aqueous, organic and ionic liquid electrolytes, bicarbonates (typically $KHCO_3$) solution has been considered a suitable electrolyte by the merits of excellent CO_2 affinity as well as readily pH-buffering and proton donation capabilities [28]. However, $KHCO_3$ solution with 0.1–1 M
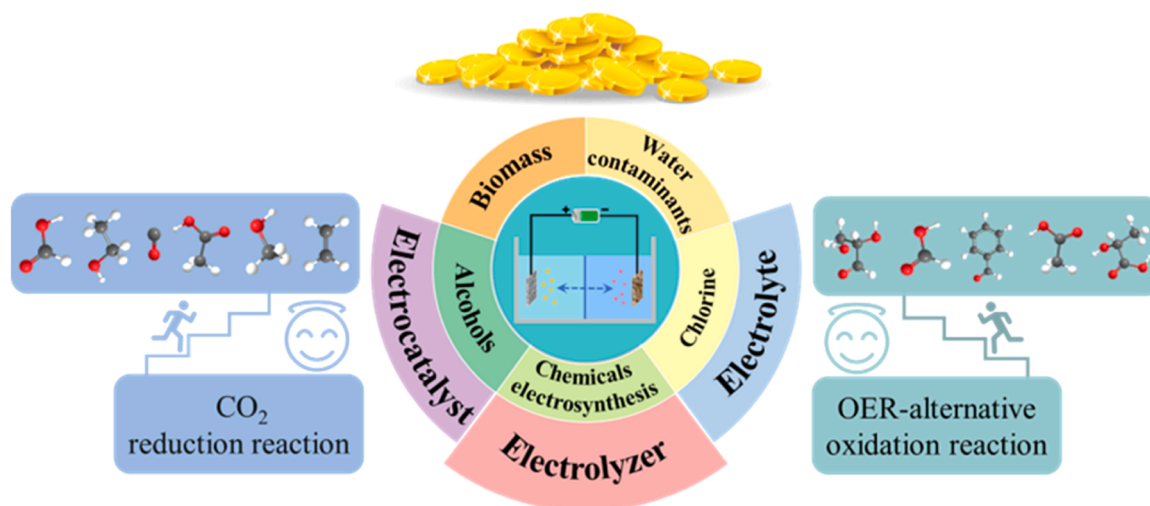
Fig. 1. Schematic illustration of the integrated system of electrochemical CO_2 reduction coupled with alternative oxidation reactions: electrocatalysts, electrolytes, and electrolyzers.

concentration has low conductivity of 9.7–75 mS cm^{-1} [29], which will increase electrical energy consumption induced by large ohmic losses. Fortunately, the use of hydroxides electrolyte with high conductivity (201 mS cm^{-1} for 1 M KOH) provides opportunities for the function of the flow cell to deliver higher current density. In addition, the strong alkalinity of hydroxides inhibits competitive hydrogen evolution reaction (HER) to some extent [25]. Nevertheless, the problems caused by the use of hydroxides electrolyte in experiments should not be ignored. For example, the formation of HCO_3^- and CO_3^{2-}/HCO_3^- from the reaction of OH^- with CO_2 can cause irreversible acidification of electrolytes, increase cell resistance, block gas diffusion channels, as well as increase operation cost by the consumption of CO_2 and electrolytes [30]. Besides, chlorides and sulfides are sometimes used as aqueous electrolytes. The presence of chloride ions can lead to anodic chlorine oxidation reaction with the characteristics of fast reaction kinetics and high product value compared with OER [31]. Meanwhile, chloride ions also can promote the protonation of adsorbed species during cathodic CO_2 reduction [25]. Similarly, the presence of sulfide is usually accompanied by an advanced oxidation process by the generation of highly active $SO_4^{\bullet-}$ species, which participate in some anodic processes that are difficult to be oxidized and degraded, especially the oxidation of water contaminants [32]. Hence, the compositions of the catholyte and anolyte are usually different to fulfill the specific requirements of cathodic and anodic reactions. Probably, the penetration of ions may occur and then has a great impact on the redox reactions. Consequently, the electrolytes in two half chambers should be carefully selected and the effects of their components on the electrochemical performance should be systematically investigated to make the overall integrated system more efficient.

Apart from electrocatalysts and electrolytes, different types of electrolyzers equipped with various IEMs act as a key link to construct the overall electrolysis system. At present, the electrolyzers involved in the reported integrated system mainly include H-type cell [33], flow cell [34], microfluidic flow cell [35], and zero-gap cell [36]. To surmount the mass transport limitation inherent to the H-type cell, gas diffusion electrode (GDE) assembled electrolyzer is often functionalized to reduce the distance between the reactants and the catalysts, as well as accelerate the mass transfer rate and thus enhance the current density of the whole coupled system. The zero-gap cell, consisting of a cathode GDE and anode as well as an IEM pressed between them, can achieve a large mass transfer limit and obtain a large current density owing to the realization of the near-zero gap between the cathode and anode [37]. Excitingly, innovative series systems are also designed to electro-synthesize fine chemicals and compounds. For instance, ethylene was firstly generated from CO_2 reduction through a CO_2-to-ethylene

membrane electrode assembly (MEA) and subsequently injected into an ethylene-to-ethylene oxide flow cell using chloride as a redox medium at the anode to finally produce ethylene oxide, achieving outstanding performance with about 70% FEs and about 97% product specificities at ampere-level current density [38].

Commonly used IEMs are anion exchange membranes (AEM), cation exchange membranes (CEM), and bipolar membranes (BPM) [39]. Because of the different penetration capabilities of ions, the selection of IEM has a far-reaching impact on the performance of the electrolyzer. The resistance and ion diffusion paths due to different thicknesses of IEM and compositions in the membrane will also affect the current density of the electrolysis system [39]. Significantly, the crossing of products through IEM during electrochemical reactions may leads to pH variation, membrane deactivation and electrode failure [40]. With high ion conductivity, CEM is widely used in H-type cells for CO_2RR but suffers from swelling and alcohols crossover issues. AEM is frequently used in flow cell, especially in KOH electrolyte to suppress HER for CO_2RR but suffers from transport of negatively charged species including CO_2RR products (e.g. $HCOO^-$ and CH_3COO^-) and reactants (e.g. OH^-, HCO_3^- and CO_3^{2-}). It is worth noting that, on the one hand, the crossover issues lead to the FE underestimation of CO_2RR products, and on the other hand, the species delivered to the anode may compete with the oxidation reactions. In addition to preventing the migration and crossover of ions and products, BPM also makes good use of water dissociation to match cathode and anode with different electrolytes [41]. Nevertheless, the cell voltage of the BPM equipped cell is higher than that of the AEM due to the high overpotential required for water dissociation. From the perspective of economic feasibility, these problems will cause an increase in the maintenance cost and production cost of CO_2RR electrolyzer, making the system less economically feasible. Therefore, the establishment of an excellent CO_2RR precipitated integrated system requires high-performance catalysts, appropriate electrolytes, exquisite electrode assemblies and suitable electrolyzer configurations.

2.2. Energy efficiency (EE)

EE is the ratio of the energy obtained from product generation to the input energy of the overall integrated system, which is proportional to Faraday efficiency (FE) and the ratio of the thermodynamic cell voltage to the operating cell voltage [42]. Therefore, high FE and low operating cell voltage are indispensable for higher EE. As a valuable evaluation criterion, EE should be greater than 70% for a technology to be economically effective [43]. Nevertheless, the traditional CO_2RR||OER system gives a quite low EE value because OER consumes almost 90% of

the energy input. Thereby, it is very necessary to find an applicable anode reaction instead of OER coupled to CO_2RR to achieve energy saving and maximally add up value to the final products.

2.3. Value-added products

Converting CO_2 and other low-value substrates or even wastes into value-added products has created significant economic benefits. For cathodic CO_2RR, gaseous CO_2 can be converted into multiple carbon-containing products of high value (e.g. CO, HCOOH, CH_3OH, CH_3CH_2OH and C_2H_4), which hold considerable potential applications as renewable fuels and chemical feedstocks [44]. Meanwhile, the inevitable occurrence of electron-competitive HER poses a stern challenge to the selectivity of carbon-containing products. On the anode side, OER-alternative reactions have also produced many kinds of high value-added products compared to low-value O_2, such as glyceralde-hyde, benzaldehyde, furan carboxylic acid, and chlorine gas [24]. For example, as the most abundant monosaccharide from cellulose-rich and starch-rich biomass, the glucose can be electrocatalytically oxidized into HCOOH, gluconate, glucuronate, and glucarate, serving as key intermediates with growing demand in biodegradable polymers and pharmaceuticals production [45]. However, the generation of high-value products from anodic reactions generally suffers from low yields with relatively low selectivity. Noteworthily, the competition between OER and desirable alternative oxidation reactions causes tricky problems with product selectivity and purity. Considering the market-entry barriers, the unsatisfactorily selective production of valuable chemicals at two sides of the integrated system will increase the separation cost of downstream target-specific products, thus reducing the economic value of the entire system [12]. Therefore, controlling and the highly selective generation of specific value-added products is very important for economic feasibility but also put forward higher requirements for the design of the integrated system.

2.4. Tech-economic analysis

Tech-economic analysis (TEA) is an important reference index to determine the performance parameters that must be realized when the system reaches economic feasibility [46]. Taking the capital input, operating costs, and the product market potential of the CO_2 electrolytic system into account, a TEA found that products are economically viable only if they are CO and HCOOH in the current economic environment [47]. And it also indicated that ethanol, n-propyl alcohol, and other high-order alcohol products would show economic feasibility when the current density, overpotential and FE severally exceeds 300 mA cm^{-2}, 500 mV, and 70%. Sometimes, CO_2 electrolytic systems have been criticized for the high production costs relative to market prices due to the high energy-consuming anodic OER [48]. Remarkably, a recent TEA study demonstrated that coupling CO_2RR with anodic glycerol oxidation reaction reduced the power consumption of the system by 53% compared to $CO_2RR||OER$ pair [49], which will further improve the economic viability of CO_2 utilization. Furthermore, a study cash flow analysis highlighted that coupling CO_2RR with organic oxidation reactions (ORR) is economically feasible after automatically screening 295 possible CO_2RR–OOR combinations [12], further proving the importance of reasonable coupled systems.

TEA provides guidance for the selection of novel anodic reactions to pair CO_2RR, promoting the integrated systems from laboratory to commercialization. When evaluating economic benefits, several key indicators such as reactants supply cost, electrolysis system cost, and product market price and size should be considered. Each key indicator is affected by many critical factors. For example, factors that affect the electrolysis system cost include electrolyzer type, electrocatalyst, membrane, electricity consumption, productivity and product separation. Noteworthily, the product separation cost and feedstocks cost are usually neglected. Kibria et al. [46] apply a CO_2 cost of $40 t^{-1} based on

amine CO_2 capture technology and separation cost of $60 t^{-1} for liquid CO_2RR products based on the Sherwood plot. Comparatively, Zhu et al. [50] estimated the separation cost of formate and ethanol to be $880 t^{-1} and $380 t^{-1}, respectively, according to a distillation cost model. Obviously, TEA results vary enormously based on different models. Current studies generally establish a simplified model to conduct TEA [51,52], but only for the cathodic CO_2RR, without considering the anode counterpart. Therefore, a reliable TEA for the overall integrated system considering both anode and cathode sides is particularly important and urgently needed to ensure the economic feasibility for realizing the commercialization and industrialization of CO_2RR technology. Given the complexity in which key indicators must be considered together rather than individually, machine learning can be recommended as an efficient way to conduct TEA.

3. Integrated systems of CO_2RR with OER-alternative oxidation reactions

To date, several anodic reactions have been developed to replace OER with CO_2RR, including alcohols oxidation, biomass oxidation, chlorine oxidation, wastewater contaminants oxidation, and chemical electro-synthetic reactions. In this section, the influencing contributions concerning electrocatalysts, electrolytes, and electrolyzers assemblies on the performance of the aforementioned integrated system are discussed in detail. Table 1 summarizes the representative components covering electrocatalysts, electrolytes, electrolyzers and products with corresponding selectivity in recently reported integrated systems. Moreover, special emphasis is paid to the use of additional energy assistance of light and thermal as well as the ingenious design of series cell/reaction to system performance improvement.

3.1. CO_2RR coupled to alcohol oxidation reaction ($CO_2RR||AOR$) integrated systems

Among several types of OER-alternative anodic oxidation reactions, alcohol oxidation reaction (AOR) is the most readily option to combine with CO_2RR, including the oxidation reactions of methanol (MOR) [14, 15,53–66], glycerol (GOR) [49,67–71], ethanol (EOR) [66], ethylene glycol (EGOR) [72], propanediol [73] and aromatic alcohol [74,75]. The low oxidation potential of alcohols can greatly decrease the cell voltage of the electrolysis system to enhance overall EE. Moreover, carbonyl or carboxyl compounds as selective oxidation products of alcohols usually are significant intermediates of chemical products with substantial economic value [76]. A combination of cathodic CO_2-to-CO with anodic propanediol oxidation to lactic acid presents a great economic attractiveness by a 0.22 €/kWh product value with a four times increasement over the $CO_2RR||OER$ system [73]. Therefore, the $CO_2RR||AOR$ integrated system for anodic and cathodic co-production of high-value chemicals is of great interest to researchers.

3.1.1. Thermodynamic feasibility

It can be seen from Table 1 that CO and HCOOH are the main products from cathodic CO_2RR in the reported $CO_2RR||AOR$ integrated systems. A cradle-to-gate evaluation shows that the economic viability of CO_2RR can be improved by significantly reducing the operating cost and CO_2 emission of the integrated system if the electrolysis voltage is lowered [49]. Table 2 shows the calculated Gibbs free energy for the reaction ($\triangle_r G^0$) and the standard thermodynamic cell potential ($|U_{cell}^0|$) values for selected combinations of $CO_2RR||AOR$ based on one mole of CO_2. Obviously, the vast majority of the overall energy consumption come from OER and $CO_2RR||AOR$ electrolysis can significantly reduce $|U_{cell}^0|$. For instance, the $|U_{cell}^0|$ value for the paired redox reactions of CO_2RR to CO or HCOOH in tandem with anodic MOR to HCOOH are 0.11 and 0.23 V, respectively, with remarkable reduction by 91.7% and 84.1% compared to that of $CO_2RR||OER$ counterparts ($|U_{cell}^0|$ value of 1.33 and 1.45 V, respectively). In fact, the $CO_2RR||MOR$ paired system

Table 1

A summary of the integrated CO_2RR systems with anodic alcohols, biomass and chlorine oxidations concerning electrocatalysts, electrolyte, electrolyzer, membrane, cell voltage, major products and corresponding maximum FEs for cathodic and anodic reactions.

Cathode catalyst	Catholyte	Cathode product (FE$_{max}$/%)	Anode catalyst	Anolyte	Anode product (FE$_{max}$/%)	Cell voltage [V]	Cell type (membrane)	Ref
Pd/MnFe$_2$O$_4$	2.0 M KHCO$_3$	HCOOH (97.5%)	Pd/MnFe$_2$O$_4$	0.5 M KOH + 400 mmol CH$_3$OH	CO$_2$ (N/A)	N/A	H-type cell (PEM)	[14]
Ni&NiNC	1 M KOH	CO (>90%)	Ni-MOFs@ 350	1 M KOH + 1 M CH$_3$OH	HCOOH (>90%)	2.74 V at 100 mA cm^{-2}	flow cell (N/A)	[15]
Bi-ene(BDC) @CP	0.5 M KHCO$_3$	HCOOH (~100%)	Ni-NF-AF	1 M KOH + 0.5 M CH$_3$OH	HCOOH (~100%)	2.13 V at 10 mA cm^{-2}	H-type cell (BPM)	[53]
3D Bi-ene-A/ CM	1 M KHCO$_3$	HCOOH (91.4%)	Ni(OH)$_2$/NF	1 M KOH + 0.5 M CH$_3$OH	HCOOH (97.9%)	2.303 V at 10 mA cm^{-2}	flow cell (BPM)	[54]
CuSn-4	0.5 M KHCO$_3$	HCOOH (93.7%)	CuSn-4	1 M KOH + 1 M CH$_3$OH	HCOOH (99.1%)	3.0 V at 100 mA cm^{-2}	H-type cell (PEM)	[55]
HOD-Cu	0.5 M KHCO$_3$	HCOOH (58%)	HOD-Cu	1 M KOH + 1 M CH$_3$OH	HCOOH (88%)	2.18 V at 10 mA cm^{-2}	H-type cell (BPM)	[56]
Bi-NSs	0.5 M KHCO$_3$	HCOOH (94%)	Co(OH)$_2$ @HOS/CP	1 M KOH + 6 M CH$_3$OH	HCOOH (≈100%)	2.44 V at 10 mA cm^{-2}	H-type cell (BPM)	[57]
PCN-601	0.5 M KHCO$_3$	CO (~100%-light)	PCN-601	1 M KOH + 0.1 M CH$_3$OH	HCOOH (>90%-light)	1.99 V at 5 mA cm^{-2}	H-type cell (CEM)	[58]
Ni-SAs @FNC	0.5 M KHCO$_3$	CO (>80%)	NiCo-NF-ET	1 M KOH + 0.5 M CH$_3$OH	HCOOH (~100%)	1.94 V at 10 mA cm^{-2}	H-type cell (BPM)	[59]
Ni-2CBpy^{2+}- COF	0.5 M KHCO$_3$	CO (~100%-light)	Ni-2CBpy^{2+}-COF	1 M KOH + 1 M CH$_3$OH	HCOOH (97%-light)	1.9 V at 12.65 mA cm^{-2}	H-type cell (PEM)	[60]
mSnO$_2$/CC	1 M KHCO$_3$	HCOOH (80.5%)	CuONS/CF	1 M KOH + 1 M CH$_3$OH	HCOOH (91.3%)	0.93 V at 10 mA cm^{-2}	H-type cell (N/A)	[61]
Bi-NPs	1 M KOH	HCOOH (~100%)	Ni(OH)$_2$/NF	1 M KOH + 0.5 M CH$_3$OH	HCOOH (~100%)	N/A	flow cell (AEM)	[62]
BiPO$_4$	1 M KOH	HCOOH (~100%)	S-NiCO-LDH	1 M KOH + 1 M CH$_3$OH	HCOOH (~100%)	2.48 V at 300 mA cm^{-2}	flow cell (AEM)	[63]
InS NRS	0.5 M KHCO$_3$	HCOOH (94.2%)	(oxy)hydroxide @np-Ni$_3$P	1 M KOH + 0.5 M CH$_3$OH	HCOOH (98.1%)	2.286 V at 50 mA cm^{-2}	flow cell (BPM)	[64]
Ni@HNC	0.1 M KHCO$_3$	CO (98.7%)	Ni@HNC	0.1 M KHCO$_3$ + 0.1 M CH$_3$OH	HCOOH (N/A)	2.7 V at 11.14 mA cm^{-2}	H-type cell (CEM)	[65]
CuCO$_2$Se$_4$/ CF	0.3 M NaHCO$_3$	HCOOH (92.5%)	CuCO$_2$Se$_4$/CF	1 M KOH + 1 M CH$_3$OH	HCOOH (84.4%)	0.67 V at 15 mA cm^{-2}	H-type cell (PEM)	[66]
Ag-NP	2 M KOH	CO (99.9%)	Pt-Ru	2 M KOH + 2 M C$_3$H$_8$O$_3$	HCOOH (7.2%)	− 1.5 V at 94.67 mA cm^{-2}	flow cell (AEM)	[49]
Ag-NPs	2 M KOH	CO (N/A)	Ni$_x$M$_{1-x}$/C (M=Bi,Pd,Au)	2 M KOH + 2 M C$_3$H$_8$O$_3$	HCOOH (N/A)	N/A	flow cell (AEM)	[67]
BiOI/CP	0.5 M KHCO$_3$	HCOOH (92%)	Ni$_{0.33}$Co$_{0.67}$(OH)$_2$ @HOS/NF	1 M KOH + 0.1 M C$_3$H$_8$O$_3$	HCOOH (90%)	1.74 V at 10 mA cm^{-2}	flow cell (PEM)	[68]
NiSAs/FN- CNSs/CP	2 M KOH + 2 M KHCO$_3$	CO (>90%)	CoSe$_2$/CC	2 M KOH + 2 M C$_3$H$_8$O$_3$	HCOOH (~90%)	1.97 V at 100 mA cm^{-2}	flow cell (CEM)	[69]
BiOBr	1 M KOH	HCOOH (96%)	NixB	1 M KOH + 1 M C$_3$H$_8$O$_3$	HCOOH (45%)	N/A	flow cell (PEM)	[70]
CNT-CoPPc/ CP	0.5 M HCO$_3^-$/ CO$_3^{2-}$	CO (46%)	STEMPO /mesoITO	0.5 M HCO$_3^-$/CO$_3^{2-}$ + 50 mM C$_3$H$_8$O$_3$	glyceraldehyde (83%)	N/A	H-type cell (AEM)	[71]
CuCO$_2$Se$_4$/ CF	0.3 M NaHCO$_3$	acetate (92.2%)	CuCO$_2$Se$_4$/CF	1 M KOH + 1 M C$_2$H$_5$OH	acetate (71.4%)	0.73 V at 15 mA cm^{-2}	H-type cell (PEM)	[66]
SnO$_2$	1 M NaHCO$_3$	HCOOH (70%)	NiCo$_2$O$_4$/CFP	1 M NaOH + 0.1 M PET hydrolysate	HCOOH (~85%)	1.9 V at 20 mA cm^{-2}	H-type cell (AEM)	[72]
Au/C	0.2 M KHCO$_3$	CO (~80%)	CF	0.5 M KHCO$_3$ + 0.5 M K$_2$CO$_3$ + 20 mM ACTTEMPO + 20 mM propanediol	lactic acid (~80%)	2.53 V~2.63 V at − 15 mA cm^{-2}	flow cell (AEM)	[73]
Ru molecular catalyst	0.5 M CH$_3$COOH + 0.5 M Na$_2$SO$_4$	CO (10%~14%)	Surface-bound molecular catalyst	0.1 M benzyl alcohol + 1 M CH$_3$COOH + 0.5 M Na$_2$SO$_4$	benzaldehyde (70.8%)	N/A	H-type cell (AEM)	[74]
Cu-In	0.5 M NaHCO$_3$	CO (>70%)	Pt	0.5 M NaHCO$_3$ + 0.2 MTEMPO + 0.25 M 1-phenylethanol	acetophenone (~95%)	− 0.70 V at ~3.7 mA cm^{-2}	H-type cell (PEM)	[75]
BiO$_x$	0.5 M KHCO$_3$	HCOOH (81%)	NiO NPs	0.5 M KHCO$_3$ + 10 mM HMF	FDCA (~13.1%)	2.5 V at 2 mA cm^{-2}	H-type cell (PEM)	[77]
PdOx/ZIF-8	0.5 M [Bmim] BF$_4$ + CH$_3$CN + 1.0 M H$_2$O	CO (97%)	PdO	0.5 M H$_2$SO$_4$ + 6.0 M CH$_3$CN + H$_2$O + 20 mM HMF	HCOOH (64.3%)	N/A	H-type cell (PEM)	[78]
TBP-CoPc /CNTs	0.1 M KHCO$_3$	CO (96.9%)	Py-TEMPO/CNTs	0.2 M Na$_2$CO$_3$ + 5 mM HMF	FDCA (90.8%)	N/A	H-type cell (PEM)	[79]
Sn/C	1 M KOH	HCOOH (~75%)	Ni-P @ Ni/CF	1 M KOH + 15 mM HMF	FDCA (~77%)	N/A	flow cell (AEM)	[80]

Table 1 (*continued*)

Cathode catalyst	Catholyte	Cathode product (FE$_{max}$/%)	Anode catalyst	Anolyte	Anode product (FE$_{max}$/%)	Cell voltage [V]	Cell type (membrane)	Ref
Bi-MOFs	0.1 M KHCO$_3$	HCOOH (95.6%)	Ni(OH)$_2$/CP	0.1 M KOH + 5 mM HMF	FDCA (75%)	N/A	H-type cell (BPM)	[81]
InOOH-Ov	0.1 M KHCO$_3$	HCOOH (~90%)	InOOH-Ov	1 M KOH + 10 mM HMF	FDCA (87.5%)	N/A	H-type cell (BPM)	[18]
OMP-Ni-N-C	2 M KCl	CO (97%)	OMP-Co$_3$O$_4$	2 M KCl	ClO$^-$ (87%)	2.5 V at 20 mA cm^{-2}	Single chamber cell	[31]
Cu	1 M KHCO$_3$	C$_2$H$_4$ (44%)	Pt/C	1 M KHCO$_3$ + 1 M glucose	gluconate (>49%)	1.9 V at 100 mA cm^{-2}	MEA (AEM)	[45]
SnO$_2$	0.6 M NaCl	HCOOH (>80%)	DSA	0.6 M NaCl	Cl$_2$ (~60%)	N/A	flow cell (CEM)	[82]
Ni-CB	2 M KHCO$_3$	CO (~98.5%)	DSA	saturated KCl	Cl$_2$ (~80%)	~3.8 V at 100 mA cm^{-2}	combined electrolysis cell	[83]
Fe-SAs/N-C	0.5 M NaCl	CO (~99%)	DSA	0.5 M NaCl	ClO$^-$ (~99%)	N/A	H-type cell (PEM)	[84]
CoPc/g-C$_3$N$_4$	0.6 M NaCl	CO (90.6%)	Pt	0.6 M NaCl	Cl$_2$ (N/A)	N/A	H-type cell (PEM)	[85]
Cu	0.5 M KOH + 1.5 M sea salt + 1 mg mL^{-1} EDTA	C$_2$H$_4$ (47%)	DSA	0.5 M KOH + 1.5 M sea salt	ClO$^-$ (85%)	N/A	flow cell (AEM)	[86]

has been experimentally demonstrated to require electricity input of only 0.09 kWh to produce 1 mol HCOOH, which is more energy-saving than that of 0.22 and 0.32 kWh for individual CO$_2$RR and MOR, respectively [62]. Given low energy input as an important criterion to identify OER-substitute at the anode, replacing OER with a thermodynamically more favorable AOR is a favorable means to drive CO$_2$RR towards economic feasibility. From this consideration forth, the reactants cost and the value of the products in anodic AOR must also be considered. In comparison, cheap glycerol (about $170 t^{-1}) in surplus is more suitable as oxidation substrates than methanol (about €400 t^{-1}) at anode, whereas theproduct selectivity of GOR is more difficult to control than that of MOR. Therefore, reasonable catalyst design to obtain high-value products with high selectivity while achieving high current density with low electricity consumption through exquisite electrolytic configurations become particularly important for AOR.

3.1.2. Cathode counterpart of CO$_2$RR||AOR integrated system

As for the cathode component within CO$_2$RR||AOR system in most recently reported studies, the CO$_2$RR products are generally CO or HCOOH with high selectivity (Table 1). When the CO$_2$RR product is CO, metal-free carbon, single-atom catalysts and some specific metals are the mainly selected cathode electrocatalysts. The alloyed CuIn cathode showed good performance to deliver high FE of CO (FE$_{CO}$ > 70%) with a current density of 3.7 mA cm^{-2} in the system of CO$_2$RR coupled with 1-phenylethanol oxidation [75]. With high atom utilization, the Ni single-atom dispersed carbon nanosheets (NiSA/CNs) has been employed as an active cathode in the CO$_2$RR||GOR system [69]. Due to the remarkably enhanced active sites, this CO$_2$RR electrocatalyst gives an ultrahigh turnover frequency of 1359 h^{-1} and favorable stability for CO formation with FE$_{CO}$ > 90% for 50 h (Fig. 2a-c). Despite high atom utilization of single-atom catalysts, the tedious preparation process restricts the large-scale fabrication of catalysts. Considering that H$_2$ produced by the inevitable competing HER is easily mixed with CO, making product separation difficult, it is a good choice to control the ratio of H$_2$ and CO to obtain syngas.

When the CO$_2$RR product is HCOOH, the typically involved catalysts are Ag, Au, In, Pd, Sn, Ni and Bi because of their affordability of high selectivity. Remarkably, the two-dimensional Bi thin materials stemmed from the layered crystal structure have received much attention for the merits of low toxicity and poor HER activity, as well as rich unsaturated sites and ultra-high atomic utilization [53,57,70]. The challenges for pure metallic Bi to realize high current density, selectivity and stability

within a wide potential range in CO$_2$RR stimulate researchers to make more attempts in the morphological engineering of Bi electrocatalysts [87]. Cao et al. [53] derived an ultrathin bismuthenes from a metal-organic framework (MOF) skeleton by in-situ electrochemical conversion, providing a stable current density up to − 70 mA cm^{-2} and high HCOOH selectivity (FE$_{HCOOH}$ > 95%) over a wide potential window from − 0.78 to − 1.18 V (vs. RHE). The MOF matrix provides high specific surface area and porosity, thus increasing the accessible Bi active sites and facilitating electron transport in CO$_2$RR process. In addition, 3D nanoarchitecture grown on self-standing conductive supports offers a large electrochemically active surface area for augmented accessibility of active sites and avoids the use of adhesives for an enhanced charge mass transfer capacity, resulting in excellent CO$_2$RR performance [54]. In this regard, the integrated 3D open network (Bi/CM) assembled by interconnected Bi nanosheet arrays with a thickness of 1.5 nm on copper mesh prepared by hydrothermal treatment followed with in situ electrochemical transformation strategy is shown excellent HCOOH selectivity and partial current density for stable HCOOH production (Fig. 2d and e), suggesting the feasibility of industrial implementation toward value-added chemical and fuel conversion from CO$_2$. In addition to conventional product detection methods, operando techniques are used to reveal the underlying CO$_2$RR mechanism. The key intermediate *OCHO in the process of CO$_2$RR to HCOOH has been confirmed by in situ Raman spectroscopy (Fig. 2f). Based on the direct experimental observations, the synergic cooperation of metal In and anion S^{2-} active sites of InS nanosheets is proposed to promote *OCHO* generation with timely appearance of adsorbed hydrogen intermediate from H$_2$O dissociation to eventually boost formation productivity (Fig. 2g) [64].

At present, two-electron mediated CO$_2$RR to CO and HCOOH with selectivity close to 100% shows economic attractiveness for large-scale industrialization. Compared to expensive noble metals, transition-metal-based materials (Bi, Sn, In, etc.) are better choices for cathode. Very recently, the CO$_2$RR electrocatalyst of CuCo$_2$Se$_4$ with optimized adsorption energy to *CO intermediate was designed by Saxena et al. [66] to exhibit potential-dependent product distributions, of which preferentially generated C$_2$ products of acetic acid and ethanol with FE = 100% at low potentials from − 0.1 to − 0.3 V (vs. RHE). Unfortunately, the limiting current density impedes the yielding of ample liquid carbon products. Despite current achievements, further exploration and research focusing on versatile and high-performance CO$_2$RR electrocatalysts for multiple carbon-containing products distributing from C$_1$ to

Table 2
Theoretical $\triangle_r G^0$ and $|U^0_{cell}|$ for the cathodic electroreduction of CO_2 to CO or HCOOH coupled to anodic OER or possible AOR.

Cathode Reaction	Possible anode reaction	Overall reaction	$\triangle_r G^0$ (kJ mol^{-1})	$|U^0_{cell}|$ (V)
$CO_2 + 2 H^+ + 2e^- \rightarrow CO + H_2O$	water → oxygen $2OH^- \rightarrow H_2O + 1/2 O_2 + 2e^-$	$CO_2 \rightarrow CO + 1/2 O_2$	257.21	1.33
	methanol → formate $CH_3OH + 4OH^- \rightarrow HCOOH + 3 H_2O + 4e^-$	$CO_2 + 1/2CH_3OH \rightarrow CO + 1/2 H_2O + 1/2HCOOH$	21.31	0.11
	glycerol → formate $C_3H_8O_3 + 8OH^- \rightarrow 3HCOOH + 5 H_2O + 8e^-$	$CO_2 + 1/4 C_3H_8O_3 \rightarrow CO + 1/4 H_2O + 3/4HCOOH$	53.99	0.28
	glycerol → glyceraldehyde $C_3H_8O_3 + 2OH^- \rightarrow C_3H_6O_3 + 2 H_2O + 2e^-$	$CO_2 + C_3H_8O_3 \rightarrow CO + C_3H_6O_3 + H_2O$	98.41	0.51
	1,2-propanediol → lactic acid $C_3H_8O_2 + H_2O \rightarrow C_3H_6O_3 + 4 H^+ + 4e^-$	$CO_2 + 1/2 C_3H_8O_2 \rightarrow CO + 1/2 C_3H_6O_3 + 1/2 H_2O$	122.36	0.63
	1-phenylethanol → acetophenone $C_8H_{10}O + 2OH^- \rightarrow C_8H_8O + 2 H_2O + 2e^-$	$CO_2 + C_8H_{10}O \rightarrow CO + C_8H_8O + H_2O$	N/A	N/A
	benzyl alcohol → benzaldehyde $PhCH_2OH \rightarrow PhCHO + 2 H^+ + 2e^-$	$CO_2 + PhCH_2OH \rightarrow CO + PhCHO + H_2O$	56.91	0.29
$CO_2 + 2 H_2O + 2e^- \rightarrow HCOOH + 2OH^-$	water → oxygen $2OH^- \rightarrow H_2O + 1/2 O_2 + 2e^-$	$CO_2 + H_2O \rightarrow HCOOH + 1/2 O_2$	280.66	1.45
	methanol → formate $CH_3OH + 4OH^- \rightarrow HCOOH + 3 H_2O + 4e^-$	$CO_2 + 1/2 H_2O + 1/2CH_3OH \rightarrow 3/2HCOOH$	44.76	0.23
	ethylene glycol → formate $C_2H_6O_2 + 6OH^- \rightarrow 2HCOOH + 4 H_2O + 6e^-$	$CO_2 + 1/3 C_2H_6O_2 + 2/3 H_2O \rightarrow 5/3HCOOH$	74.24	0.38
	glycerol → formate $C_3H_8O_3 + 8OH^- \rightarrow 3HCOOH + 5 H_2O + 8e^-$	$CO_2 + 1/4 C_3H_8O_3 + 3/4 H_2O \rightarrow 7/4HCOOH$	77.44	0.40

C_{2+} are still urgently needed.

3.1.3. Anodic counterpart of $CO_2RR||AOR$ integrated system

As for the anode component within $CO_2||AOR$ systems, oxidation products from alcohols are mostly HCOOH, in addition to acetate [66], glyceraldehyde [71], lactic acid (LA) [73], benzaldehyde (PhCHO) [74], and acetophenone (ACP) [75]. In recent studies, self-supported catalysts derived from MOFs have shown surprising AOR activity and nearly 100% HCOOH selectivity, as their chemical composition and morphology, are easily adjusted to fully expose their active sites [15,53, 59]. As an example, the MOR on a free-standing NiCo-based MOF-derived anode (NiCo/NF) only requires 1.29 V to achieve a high current density of 100 mA cm^{-2} with about 346 mV lower than that of OER (Fig. 3**a and b**), and HCOOH can also be simultaneously produced with near to unity selectivity [59]. By employing Pt anode, the selectivity of 1-phenylethanol to ACP can attain ~95% in 30 min assisted by

a redox mediator (Fig. 3**c**). Moreover, using the same $CO_2RR||AOR$ system, four benzylic and aliphatic alcohols of 4-methoxybenzyl alcohol, 1-phenylethanol, ethanol and isopropanol have been successfully converted into corresponding carbonyl products with the selectivity of 84%, 93%, 91% and 78%, respectively [75]. Not limited to high-purity alcohols, AOR can also be applied for upvaluing of plastic wastes, presenting a broad utilization prospect of electrochemistry. Polyethylene terephthalate (PET) can be easily hydrolyzed to its monomer units of terephthalate acid and ethylene glycol (EG) under alkaline conditions. Given this, Wang et al. [72] has found that the FE for the conversion of EG in PET hydrolysate to HCOOH is above 90% on $NiCo_2O_4$ anode, accompanying with some glycolic acid by-products in $CO_2RR||AOR$ electrolysis process (Fig. 3**d and e**).

Interestingly, most of the anode electrocatalysts given in Table 1 are transition metals including Ni, Co and Cu with the corresponding HCOOH FEs approaching 100%. Referring to MOR on CuSn catalysts, the operando Raman characterization confirms the $*OCH_3$, $*OCH_2$, and $*OCHO$ key intermediates for the formation of HCOOH from CH_3OH (Fig. 3**f**) [55]. Moreover, Luo and Fu research group has illustrated that the electrochemically formed transition metal oxyhydroxides (such as NiOOH, CoOOH and FeOOH) active centers with optimized electronic configuration have appropriate Gibbs free energy behavior for the above-mentioned intermediates from CH_3OH to HCOOH as well as a higher energy barrier to inhibit further oxidation to CO_2 through systemically density functional theory (DFT) studies [88–90]. Differently, Chen et al. [91] claimed that the AOR activity on Ni anode was predominately controlled by the lattice oxygen through an electrically generated catalyst dehydrogenation reaction with following spontaneous nucleophile dehydrogenation process. This collision of different viewpoints motivates researchers to deeply explore the underlying mechanisms concerning highly selective alcohol oxidation to valuable chemicals. More importantly, the anode catalyst must be carefully designed to prevent overoxidation of alcohols to CO_2.

Currently, MOR is the most chosen anodic reaction paired to CO_2RR as methanol is the simplest alcohol and the selectivity to HCOOH is nearly 100%. The coproduction of HCOOH on both sides of $CO_2RR||$ MOR system provides convenience for subsequent product separation and purification. Pure HCOOH can be obtained by distillation or potassium diformate can be obtained by concentration and crystallization of the catholyte and anolyte mixture after removing HCO_3^- ions. Nevertheless, methanol as a green fuel is also a desirable CO_2RR product. Without cheap access to methanol as oxidation substrates, it is questionable whether the $CO_2RR||MOR$ system is economically viable. Comparatively, GOR to convert the cheap diesel byproduct glycerol into high-value products would be a good choice for anode reaction. In view of this, it is suggested to design transition metal catalysts to achieve high product selectivity of GOR. Besides, coupling EGOR from hydrolyzed PET waste plastic with CO_2RR enables simultaneous clean energy production and waste valorization. It is also worth noting that the competitive cathodic HER and anodic OER are unavoidable for $CO_2RR||$ MOR integrated system. Since HER and OER are potential-dependent, the interference of H_2 and O_2 on the valuable products can be controlled by adjusting the cell voltage to further improve EE of the integrated system.

3.1.4. Bifunctional electrocatalysts and solar-energy assistance

In conjunction with the advantages of CO_2RR and AOR, it is of great significance to develop cost-effective and high-performance bifunctional materials. Taking this into account, Metal-based (HOD-Cu [56], CuSn [55], Pd/MnFe$_2$O$_4$ [14], CuCo$_2$Se$_4$ [66]) and carbon-supported (Ni@HNC [65] and PCN [58]) electrocatalysts have been reported in pioneering works. A graded bifunctional CuSn alloy was designed for efficient HCOOH coproduction via cathodic CO_2RR and anodic MOR, reaching a record production rate of 3313 μmol h^{-1} cm^{-2} with HCOOH selectivity approaching 100% on both sides [55]. In view of the requirements of CO_2RR catalysts, Cu-based materials can be selected as
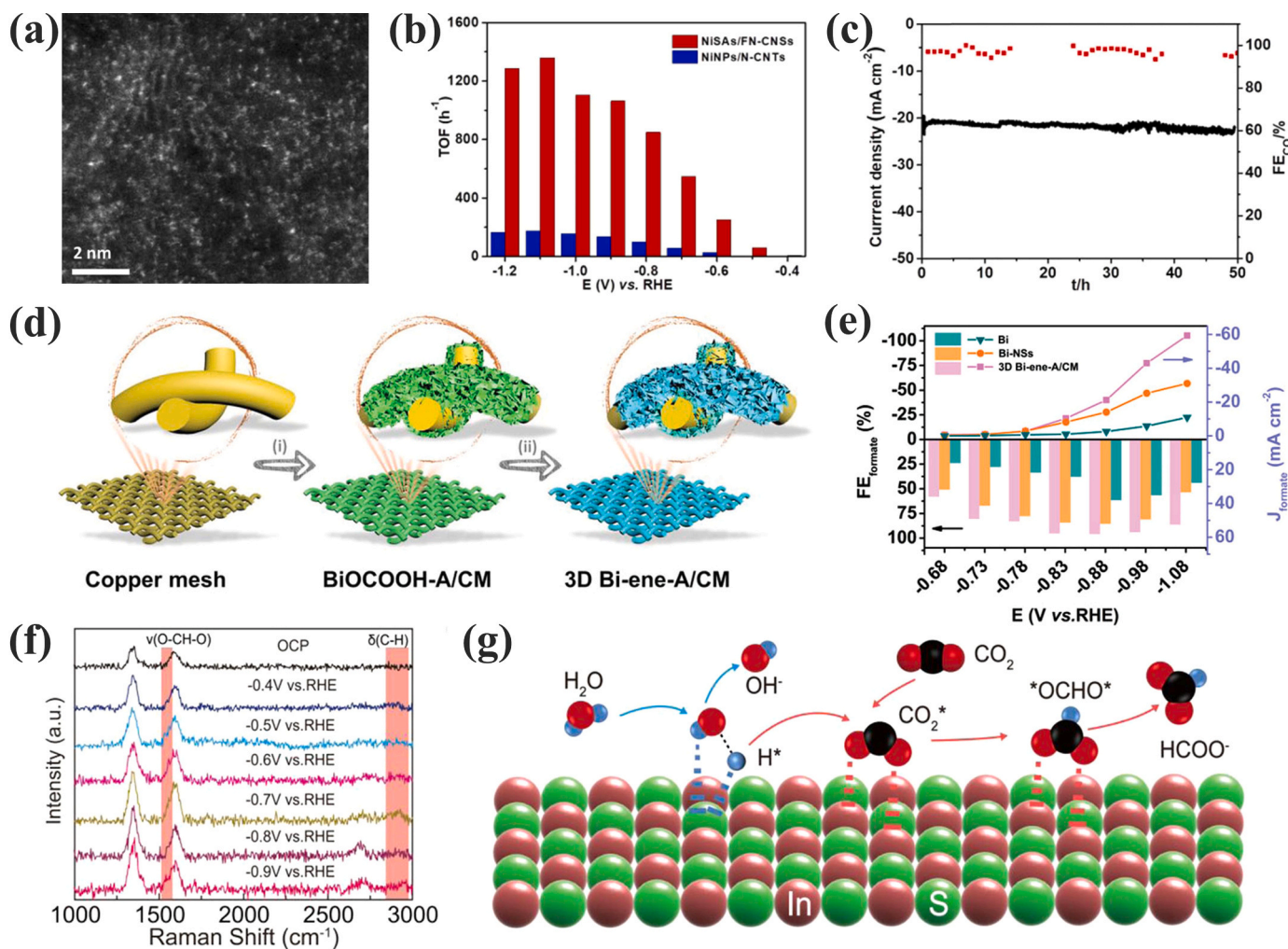
Fig. 2. Cathode counterpart of CO₂RR||AOR integrated system. (a) The HAADF-STEM image, (b) turnover frequency of CO and (c) duration test at − 0.8 V (vs. RHE) for NiSA/CNs cathode [69]. (d) Synthesis diagram and (e) $FE_{formate}$ and $J_{formate}$ for 3D Bi/CM cathode [54]. (f) Operando Raman spectra under different cathodic potentials and (g) diagrammatic drawing of CO₂RR to formate products on InS nanosheets cathode [64].

bifunctional catalysts for CO₂RR||MOR integrated systems in future studies.

Supplementing solar or heat energy to electrochemical reaction to surpass the conventional electrocatalytic performances is attracting increasing interest [92]. Cu as CO₂RR cathode and CuO as MOR anode derived from the same $Cu(OH)_2$ precursors were also recently reported to show good HCOOH coproduction performance [56]. Exhilaratingly, the anode can be further adhered to a solar cell to establish a solar-driven CO₂RR||MOR integrated system without additional electricity input, realizing a 3.6% solar-to-HCOOH efficiency (Fig. 4**a and b**). In addition to the tandem photovoltaic-electrochemical device, the electrode itself is also photo-responsive to improve the electrocatalytic performance by utilizing solar energy. In this regard, a light-assisted CO₂RR||MOR system was conducted by using a photosensitive crystalline coordination compound as bifunctional catalyst. The light was demonstrated to further improve the catalytic performance to achieve anodic $FE_{HCOOH} > 90\%$ and cathodic $FE_{CO} \sim 100\%$ in the tested potential window [58]. Furthermore, photothermal-assisted coupling electrocatalysis is also established by taking the advantage of irradiation energy and external heating together [93]. Given this, a bifunctional viologen- containing covalent organic framework (Ni-$2CBpy^{2+}$-COF) has been obtained by the same research group to successfully construct a photothermal-assisted CO₂RR||AOR system, delivering excellent electrocatalytic behavior with nearly 100% selectivity at 1.9 V both for CO at cathode and HCOOH at anode [60]. Notably, this light-assisted

integrated system affords with ~31.5% overall electricity reduction in comparison with CO₂RR||OER electrolysis (Fig. 4**c**). The on-off mode testing evidences that the surface temperature of catalyst arises to 74.8 °C after 500 s light irradiation (Fig. 4**d**). According to the *in/ex-situ* experiments, the electron-transfer mediator of cyclic diquats ($2CBpy^{2+}$) can generate photothermal effect to facilitate the redox reaction kinetics, leading to overall efficiency enhancement. Indeed, photo-assisted electrocatalysis is demonstrated as a promising approach to produce value-added chemicals and fuels with additional virtue of renewable solar energy utilization beyond electrocatalysis [94,95]. Despite the photothermal-assisted electrocatalysis system being high-performance, the selectivity of desired product remains highly dependent on the catalyst materials. Moreover, the catalysts are generally made into film-formed electrode to facilitate light irradiation. Besides, the bulk electrolyte is the site for redox reactions, and the rapid thermal diffusion in the electrolyte solution results in substantial heat loss, which poses a great challenge to the design of electrolyzers that can maximize the thermal effect. Consequently, through reasonable electrode and electrolyzer design, the photothermal effect can be fully utilized to maximize the electrocatalytic performance of the integrated co-electrolysis system.

3.1.5. Electrolyzer configurations for CO₂RR||AOR integrated systems

To date, most studies on CO₂RR||AOR integrated systems are conducted in H-type cells, which provide a good platform for studying half-
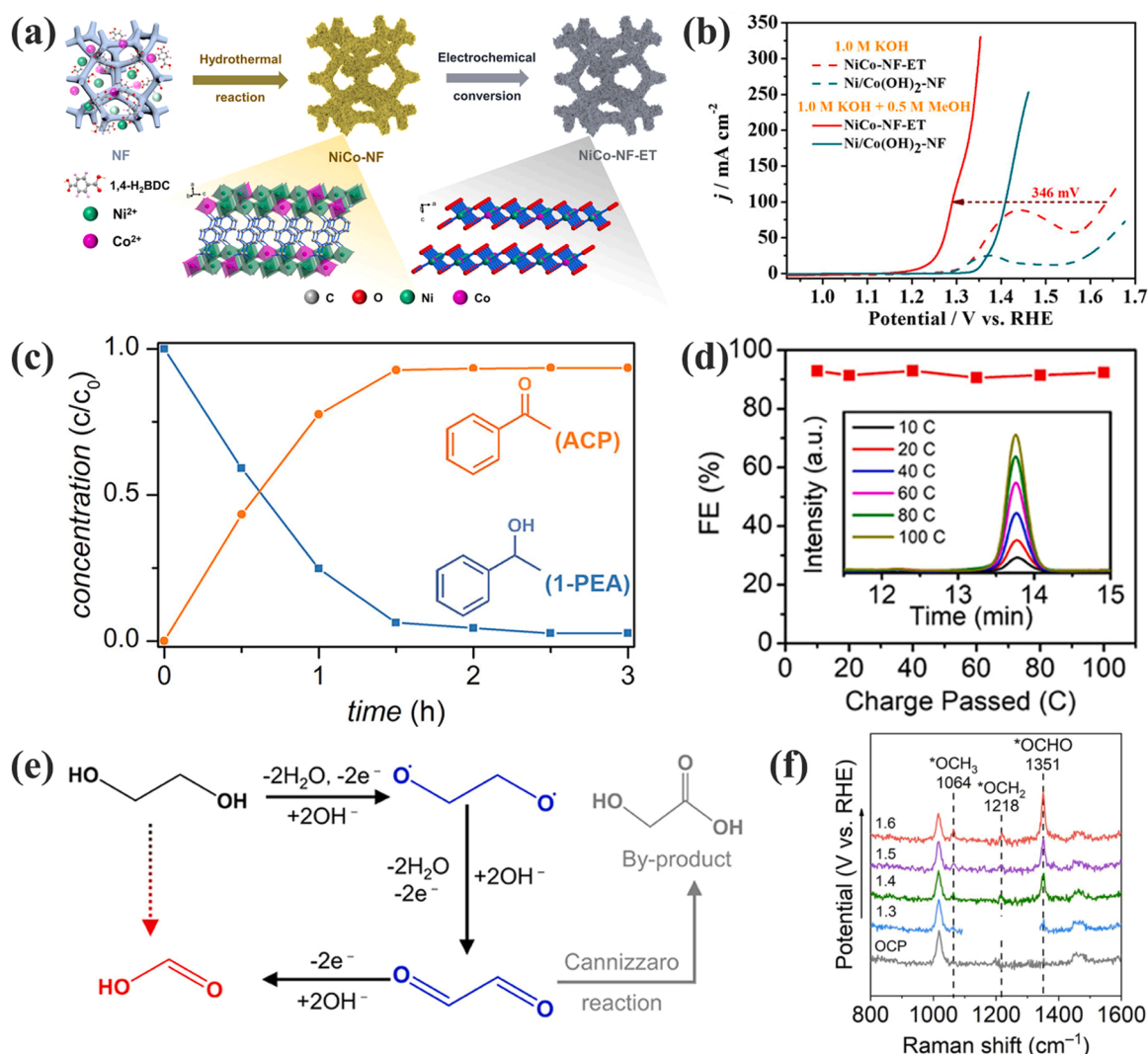
Fig. 3. Anodic counterpart of CO_2||AOR integrated system. (a) Synthetic diagram of NiCo/NF anode and (b) corresponding LSV curves in alkaline electrolyte with or without methanol addition [59]. (c) conversion efficiency of 1-PEA to ACP on the Pt anode as a function of time [75]. (d) FEs of PET hydrolyzed EG to formate as a function of charges conducted at 1.45 V with typical formate signal identified by liquid chromatography and (e) electrochemical EG-to-formate pathway on $NiCo_2O_4$ anode [72]. (f) in situ Raman spectra for MOR on CuSn alloy at different potentials [55].

reactions and corresponding catalytic mechanisms. Unfortunately, it is difficult for H-type cell to reach industrial current density because of the limited mass transmission caused by its long diffusion path (about 50 μm) [96]. Furthermore, the relatively long cathode-anode distance in H-cell results in high ohmic losses and thus high energy consumption. For this matter, the flow cell enables the utilization of alkaline electrolytes to suppress HER and therefore increase CO_2RR product selectivity by creating a high pH environment [97]. At the same time, the gas-solid-liquid three-phase interface at the GDE constituent within the flow cell breaks the mass transmission limitation and enables CO_2 reduction to be carried out at industrial-level current density. Wang et al. [69] has constructed CO_2RR||GOR system in the flow cell with continuously circulating 2 M $KHCO_3$ catholyte for CO production from CO_2RR and 2 M glycerol in 2 M KOH anolyte for HCOOH production from GOR (Fig. 4e). Amazingly, j_{CO} can achieve a stable value of 100 mA cm^{-2} at 2.2 V, accompanying with both FEs above 90% toward CO and HCOOH for ultralong durability of 400 h (Fig. 4f). This configuration only enhances CO2RR product selectivity by modifying the cathode to GDE but without any modifications to the anode. Thus, a zero-gap cathodic and anodic GDEs sandwiched MEA reactor featured with fast mass transport and small ohmic resistance is recommended to improve conversion rate and EE of the CO_2RR||MOR systems.

Typically, CO_2RR is performed with a (near-) neutral electrolyte (CO_2-saturated $KHCO_3$) in H-type cells and with a neutral or alkaline electrolyte in flow cells, whereas anode AOR applies an alkaline electrolyte (usually KOH). Since the CO_2RR and AOR require specific reaction medium and cell configuration, membrane separator is particularly important because they can influence the local chemical environment of the catalyst layer, reactant accessibility and reaction bias [40,98]. The CEM usually transports H^+ produced by the anode to the cathode, thereby resulting in a high acidic PH of the cathode, thus promoting HER to affect the activity of CO_2RR [99]. Furthermore, electrocatalyst reconstruction usually happens during the redox reactions in electrolysis, sometimes along with metal ion leakage into electrolyte [100–102]. These metal ions may pass through CEM to cause electrode poisoning or transformation by ion dissolution and redeposition on electrocatalysts, eventually altering the CO_2RR and AOR activities. Besides, proton exchange membrane (PEM) as a type of CEM with extensive usage in fuel cells, is also applied to CO_2RR||AOR system. However, the high permeability of methanol leads to the poisoning of electrodes and the degradation of system properties [103–105], which limits its application in CO_2RR||MOR system. AEM usually transports anions from the cathode to the anode, resulting in the reduction of H^+ concentration to inhibit HER for cathodic CO_2RR [106]. However, the HCO_3^- and CO_3^{2-}
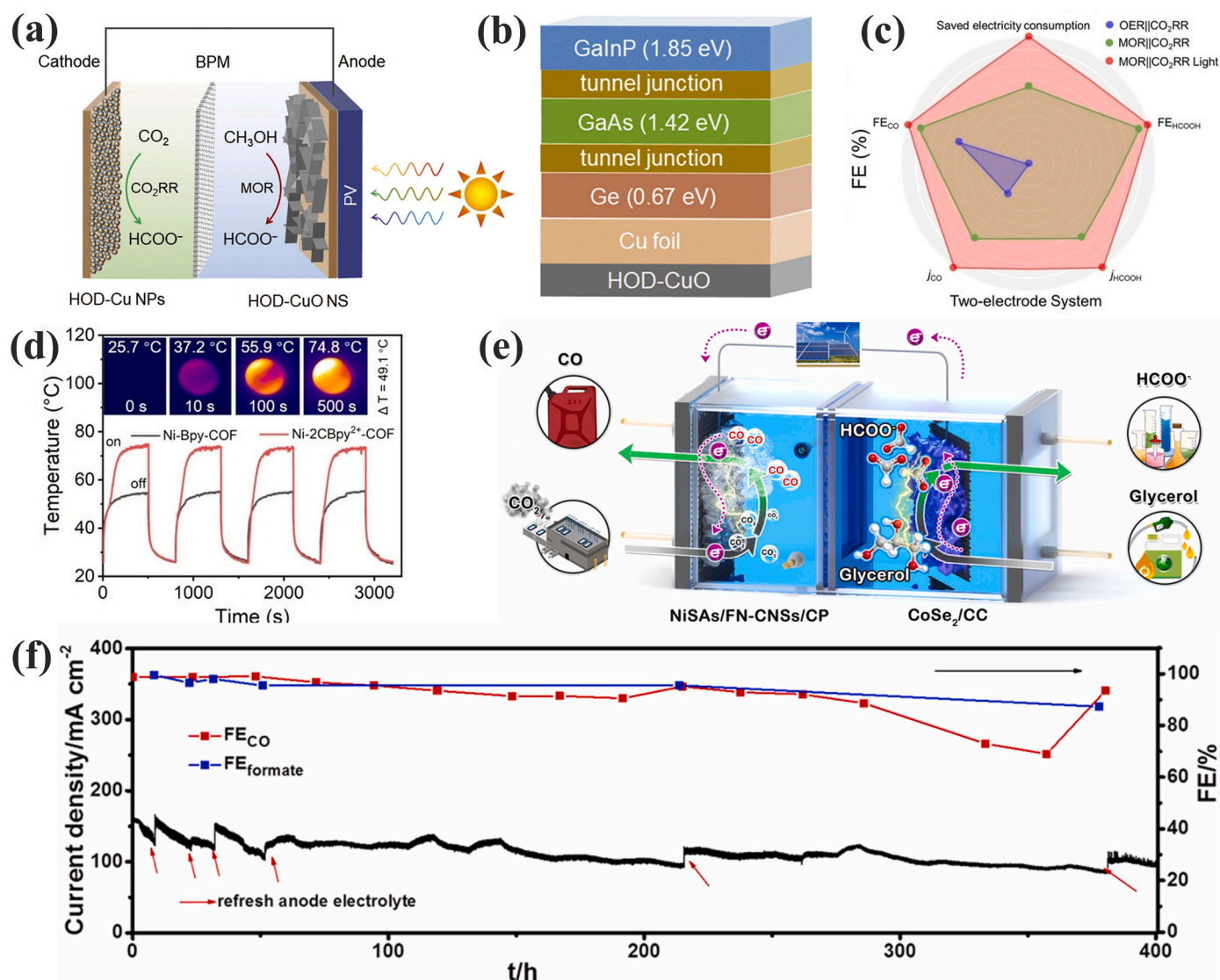
Fig. 4. (a) Schematic illustration of the solar-driven CO$_2$RR||MOR integrated system and (b) the corresponding anode structure [56]. (c) Radar chart for electrochemical activity in different integrated systems and (d) temperature changes testing at on-off mode under light irradiation and corresponding photothermal images using Ni-2CBpy^{2+}-COF as bifunctional catalysts [60]. (e) Schematic of CO$_2$RR||GOR integrated system and (f) corresponding durability test of the electrolyzer at 2.2 V [69].

generated by the reaction of CO$_2$ with the OH$^-$ produced by the cathode will probably diffuse through the membrane to the anode and further reduce the cathodic utilization rate of CO$_2$ [40]. Meanwhile, the migrated HCO$_3^-$ and CO$_3^{2-}$ at the anode will re-react with KOH electrolyte to release CO$_2$, perturbing the reaction environment for AOR. Note that HCOO$^-$ commonly seen in CO$_2$RR||AOR may also crossover AEM from cathode to anode driven by electromigration. Given that HCOO$^-$ migration rate is highly associated with the current density and catholyte flow rate [107], the quantity of HCOOH at cathode may be underestimated but with HCOOH over-estimation at anode. Consequently, the concentration of generated HCOOH in the cathode and anode should be comprehensively measured to ensure the accuracy of FE calculations. BPM maintains a different PH environment at the cathode and anode by electrolysis of water at the interface, which not only eliminates the possibility of HER but also prevents crossover of products so that it can be used in CO$_2$RR||AOR integrated system [108]. Nonetheless, due to the high overpotential and high current density caused by hydrolysis dissociation, it still suffers from poor stability [109]. Therefore, in addition to high-performance catalyst, it is suggested to construct an electrolyzer composed of cathodic and anodic GDEs to

perform CO$_2$RR||AOR integrated system at high current density and long durability.

3.2. CO$_2$RR coupled to biomass oxidation reaction (CO$_2$RR||BioOR) integrated system

Biomass as the most ideal substitute for fossil fuels has the advantages of abundant content and renewable resource mainly including plants, aquatic organisms, animal and human wastes [110,111]. In recent years, organic fuels and chemical products such as furan compounds, monosaccharides and amino acids derived from biomass have received extensive attention due to their versatility in industrial applications as valuable platform substrates [112]. Therefore, constructing CO$_2$RR||BioOR paired reactions offers a great opportunity to realize concurrent production of high value-added products.

HMF is a biomass derivative building block chemicals from monosaccharides or cellulose [113–115]. Recent estimates indicate that HMF is a high-value C$_6$ platform molecule with a market value of $55 million by 2024 [113,116]. HMF can be oxidized to generate important chemicals such as 5-hydroxymethyl-2-furancarboxylic acid (HMFCA), 2,

5-diformylfuran (DFF), 5-formyl-2-furan-carboxylic acid (FFCA), FDCA, maleic acid (MA) and HCOOH, among which FDCA is considered to be a highly valuable chemical used for the production of polyethylene fur-andiformate [117,118]. Interestingly, Yang et al. [81] used the obtained FDCA from anodic HMF oxidation to synthesize Bi-based MOF materials as CO_2RR electrocatalysts, which further expands the FDCA application prospect. HMF oxidation reaction (HMFOR) for valuable chemicals production has been widely studied by coupling with HER for highly efficient cathodic H_2 generation [119,120]. To date, there are relatively few reports on CO_2RR||HMFOR integrated system (Table 1), however, it
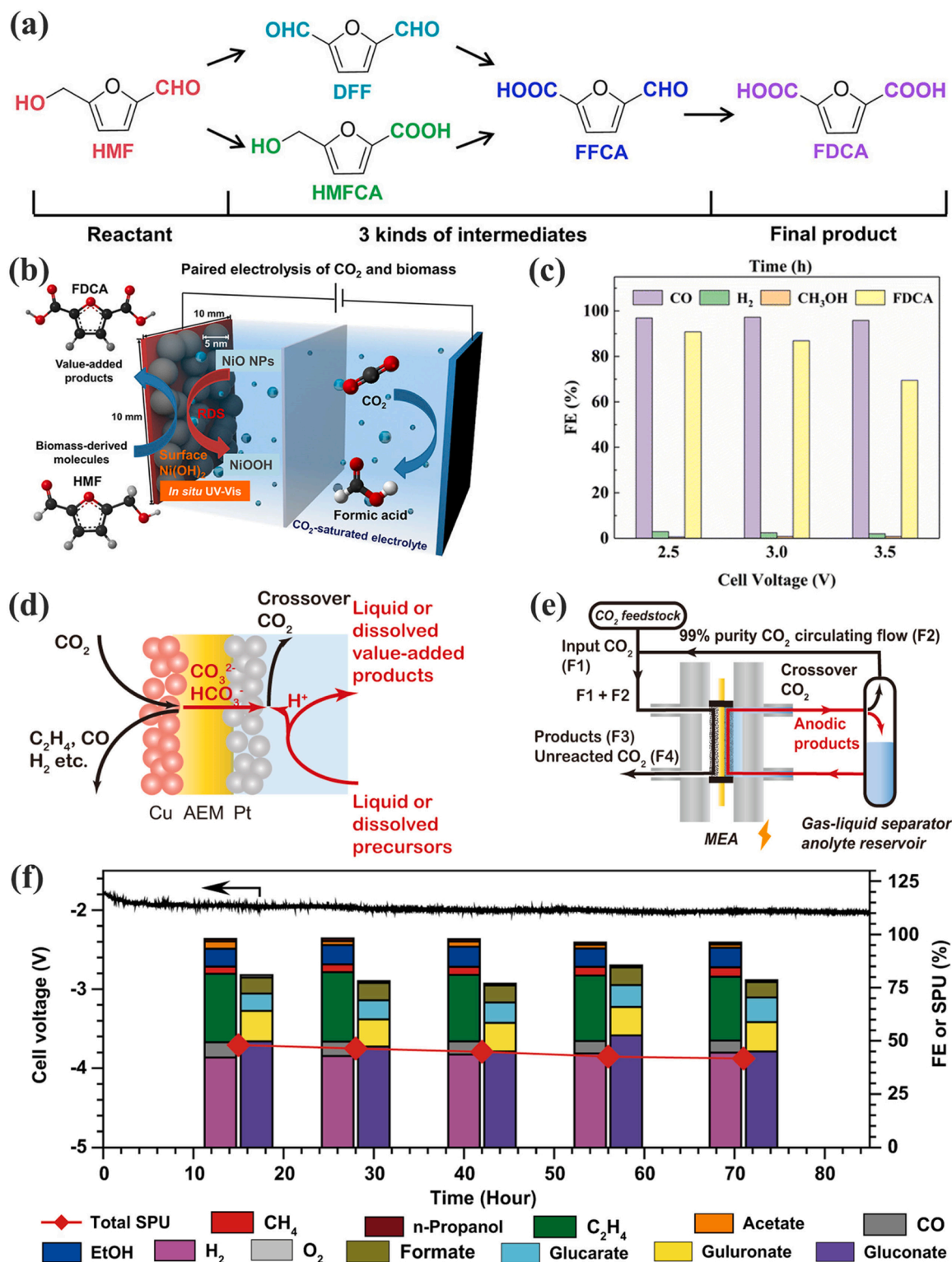
Fig. 5. (a) Proposed reaction pathways of HMF oxidation to FDCA and (b) a typical CO_2RR||HMFOR system [77]. (c) The product distribution with different FEs at different cell voltages [79]. (d) The MEA-type electrolyzer for CO_2RR coupled with glucose oxidation, (e) cell configurations with a gas recovery subassembly to recirculate the crossed CO_2 from the anode to return to the cathode and (f) Long-term electrolysis performed at a current density of 100 mA cm^{-2} with FEs of cathodic and anodic products [45].

still attracts research attention due to its obvious energy advantages and great economic value. Similar to the above-mentioned CO$_2$RR||AOR system, CO- and HCOOH-producing cathodes with high selectivity are the primary consideration in CO$_2$RR||HMFOR system. Impressively, the PdOx/ZIF cathode delivered a high CO selectivity (FE$_{CO}$ = 97%) with a high current density of 103.5 mA cm^{-2} in CO$_2$RR||HMFOR integrated system [78]. At the same time, this system used PdO anode electrolyzing HMF in a high-acid electrolyte to yield 84.3% HCOOH and MA. Since most of the previously reported anodic HMF electrolysis was carried out under near-neutral or alkaline conditions, this work provides more possibilities for the selection of anolyte. Noticeably, as one of the HMF oxidation products, FDCA is easily precipitated under high-acidic conditions [121]. FDCA precipitation will cause blockage of the membrane and electrode, which is detrimental to catalytic performance. Besides, the electrocatalysts that can stably function in acidic electrolytes are extremely limited, usually noble metal catalysts, which undoubtedly decreases the economic viability of the system. Therefore, more attention should be paid to the characteristics of the product and the applicability of the catalyst when using different electrolytes.

As for the anode of the CO$_2$RR||HMFOR system, the oxidation of HMF to specific products relates to multiple electron-transfer steps. For example, HMF-to-FDCA is a six-electron transfer process through a variety of value-added intermediates (Fig. 5a). Therefore, the design and regulation of catalysts are very important to selectively obtain desirable chemicals from HMF oxidation. In a pioneering work, Choi et al. [77] synthesized NiO nanoparticles with a diameter of 5 nm as an anode catalyst and the reported HCOOH-producing BiO$_x$ as cathodic electrocatalyst to establish a CO$_2$RR||HMFOR system (Fig. 5b). In CO$_2$-saturated 0.5 M KHCO$_3$ solution, a total 36% FE for FDCA, FFCA, DFF and HMFCA was achieved from HMF oxidation at 2 mA cm^{-2} driven by 2.5 V cell voltage. Notably, the near-neutral condition endows relatively slow oxidation of HMF [77,122], in spite of its appropriateness for CO$_2$RR. Even though high reaction rate is preferred in alkaline reaction environment for HMF oxidation, harmful humins may be produced under ultrahigh alkaline pH [123]. Thus, it is necessary to carefully balance the advantages and disadvantages of near-neutral catholyte and alkaline anolyte to construct the coupling system. Keep this in mind, an integrated system is constructed using molecular catalysts adopting CO$_2$RR in a near-neutral electrolyte and the oxidation of HMF in an alkaline electrolyte with gradient pH, achieving 90.8% FDCA selectivity and 96.9% CO selectivity at the electrolysis voltage of 2.5 V (Fig. 5c). For the first time, a solar-powered electrolysis device has been successfully applied to achieve a 95.4% CO selectivity and 69.9% FDCA yield without additional electricity input [79]. This will provide a sustainable pathway for the conversion and utilization of renewable energy in the future. Very recently, Hu et al. [18] developed an outstanding bifunctional InOOH electrocatalysts rich in oxygen vacancy for cathodic CO$_2$-to-HCOOH and anodic HMF-to-FDCA. Encouragingly, this PH-asymmetric CO$_2$RR||HMFOR integrated cell separated by BPM achieving about 90% HCOOH selectivity for the cathode and 87.5% FDCA selectivity for the anode at 2.27 V, demonstrates the importance of catalyst design and also provides a reference for other coupled reactions to generate value-added commodity chemicals. However, the slow water dissipation at the BPM interface causing the system to apply a large potential is still a non-negligible problem [41]. Besides, the inherent layering and foaming characteristics of BPM are also an impediment to the stable development of the system [124]. Thus, more powerful IEMs should be further investigated to improve the performance of the CO$_2$RR||HMFOR system.

Apart from HMFOR coupling, glucose oxidation reaction has also been reported to couple with CO$_2$RR in a MEA-type electrolyzer (Fig. 5d) [45]. As no gaseous products are generated in the anode chamber, this integrated device is designed with a gas recovery subassembly to recirculate the crossed CO$_2$ passing through the anode to return to the cathode, achieving a CO$_2$ utilization rate of 75% (Fig. 5e). Note that cathodic C$_2$H$_4$ production on Cu through CO$_2$RR is often accompanied

by ethanol, acetate, HCOOH and other liquid products permeating through the membrane to the anode, thereby causing pollution to the anode [12,125]. In this study, the researchers adjusted the reaction temperature and found that moderately high temperatures changed the evaporation rate into the cathode gas stream, thereby reducing the crossing of liquid products to the anode. Notably, this device achieves a stable synthesis of C$_2$H$_4$ product with a high value on the Cu cathode in a zero-gap MEA for over 80 h at 100 mA cm^{-2} (Fig. 5f), promoting innovative CO$_2$RR electrolysis toward industrial applications with high carbon efficiency.

So far, there are relatively few studies on CO$_2$RR||BioOR coupling electrolysis. In addition to more biomass alternatives such as cellulose, lignin and protein for selective anodic oxidations, electrosynthesis of jet fuels using biomass platform chemicals as precursors on the anode arises as a new sustainable process [126], endowing CO$_2$RR||BioOR integrated system with more options. Given the complexity of biomass, it is ideal to have a few or even one value-added BioOR product. Compared with the wide applications in CO$_2$RR, flow cells have rarely been explored for biomass valorization. Consequently, the appropriate reactor type, electrolytes and IEMs should be carefully constructed to match the specific reactions of CO$_2$RR||BioOR systems. Additionally, product-separation technology should be considered when evaluating system economics.

3.3. CO$_2$RR coupled to chlorine oxidation reaction (CO$_2$RR||COR) integrated system

Chlor-alkali reaction as one of the biggest electrosynthesis processes in the world has significant commercial value in the social economy [85, 127]. Chlorine oxidation reaction (COR) is mainly employed in the chlor-alkali industry to generate active chlorine species (Cl$_2$, HOCl and OCl$^-$). COR has a higher thermodynamic equilibrium potential (1.36 V) than OER. However, its faster kinetic advantage and high-value products still drive researchers to set up a CO$_2$RR||COR integrated system [128]. Furthermore, due to the large amount of absorbed CO$_2$ and chloride ions in seawater [129], direct CO$_2$RR||COR electrolysis in seawater shows promising prospects in seawater desalination and chemicals/fuel generation under the goal of carbon neutrality.

3.3.1. Cathodic and anodic electrodes

As for the cathode of CO$_2$RR||COR system, the main products are still HCOOH and CO produced by typical Ni, Ag, Ti and Bi involved electrocatalysts (Table 1). Utilizing N-doped carbon supported Fe single atoms as cathode, a solar cell powered CO$_2$RR||COR integrated system can accomplish excellent performance of FEco = 93% and EE = 92% at 2.0 V (Fig. 6a). This system not only achieves nearly 100% atomic utilization but also provides a reference to make full use of renewable electricity for chemical reactions [84]. Besides, for HCOOH formation, SnO$_2$ with a high energy (111) surface achieved FE$_{HCOOH}$ > 80% in the wide potential window of 0.5 V because of the stronger adsorption energy of *OCHO intermediate over HCOOH* at a high energy surface [82]. Different from the aforementioned C$_1$ products, C$_2$H$_4$ has been reported to produce on Cu surface with FE = 47% at a working current of 100 mA cm^{-2}, which is ascribed to highly-active Cu dendrites induced by dissolution and deposition on Cu surface through adding EDTA to the sea salt electrolyte [86].

As for the anode of CO$_2$RR||COR system, commercial dimensionally stable anodes (DSA) assembled by precious metal oxides (e.g. RuO$_2$ and IrO$_2$) on Ti substrate are the predominate COR electrocatalysts due to its anti-corrosion property [128]. Owing to the scarcity of precious metals, researchers have attempted to explore non-precious anodes for the development of the CO$_2$RR||COR integrated system. Ge et al. [31] have recently developed ordered mesoporous Co$_3$O$_4$ catalysts to achieve more than 80% ClO$^-$ production at the anode at a current density of 70 mA cm^{-2} in a single cell with only 3.0 V cell voltage. Techno-economic evaluations suggest that the energy cost minimizes to 31.5 $ kWh^{-1} at an ultra-low cell voltage of 2.5 V at 20 mA cm^{-2} in a
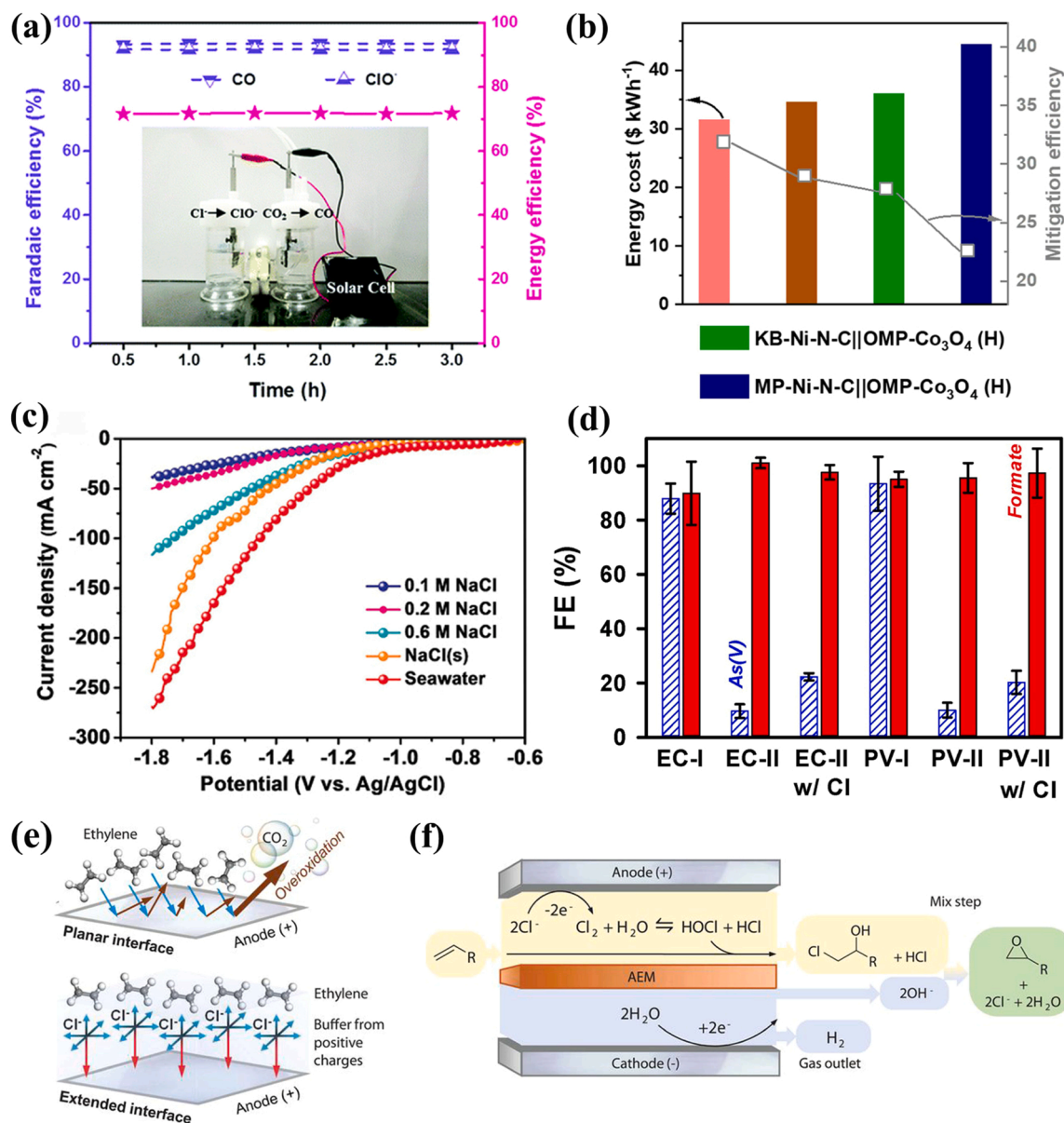
Fig. 6. (a) EE and FEs of CO and ClO⁻ in a solar cell powered CO₂RR||COR integrated system [84]. (b) Techno-economic evaluations for a H-type CO₂RR||COR integrated system at 20 mA cm⁻² in 2.0 M KCl [31]. (c) LSV curves of CO₂RR cathode in different concentration of NaCl solution and natural seawater [85]. (d) FEs for As (V) and formate formation in different electrocatalytic (EC) or photovoltaically assisted electrocatalytic (PV) integrated systems [130]. (e) Comparative schematic illustrations of ethylene oxidation at planar and extended interfaces and (f) Schematic illustration for the electrosynthesis of ethylene oxide system using C₂H₄ generated from a conventional CO2RR||OER electrolysis system as reactants and highly-active species from COR to trigger the series oxidation reactions [38].

H-type CO₂RR||COR integrated system (Fig. 6**b**). The authors also pointed out that the single cell showed high current density accounted for the short electron transport path but awful stability owing to the corrosion of ClO⁻ on the electrode. However, ClO⁻ and Cl⁻ may diffuse to the cathode through the AEM, thereby corroding the cathode electrode and affecting the FE of the anode product. Therefore, special attention should be paid to the selection of IEMs and electrodes when constructing CO₂RR||COR systems.

3.3.2. Electrolysis configuration design

The electrolyte compositions greatly affect the performance of overall CO₂RR||COR system. The effects of different concentrations of NaCl and natural seawater on CO₂RR||COR system have been investigated. LSV curves in Fig. 6**c** demonstrate that natural seawater delivers the highest current density for CO₂RR due to its high ionic conductivity [85]. Considering the existence of a variety of ions in seawater leading to

the generation of precipitation on the electrode, pure NaCl solution is usually adopted to simulate seawater reaction environment and showed better stability compared with the traditional NaHCO₃ electrolyte [85, 131]. Apart from the typical CO₂RR||COR electrolysis, some specific integrations have been designed to make use of the generated highly oxidative chlorine species from the COR reaction. Choi et al. [130] designed a photovoltaic system coupling chlorine-mediated CO₂RR with As(III) oxidation by taking advantage of the high oxidation ability of active chlorine species to realize maximal FE = 95% for reactions on both sides (Fig. 6**d**), providing an interesting idea for efficient toxic As (III)-containing wastewater treatment. Loew et al. [38] postulated that a redox mediator can promote the indirect exchange of electrons between the electrode and the substrate molecules for selective oxidation of the organics (Fig. 6**e**). Following this proposal, a C₂H₄-to-ethylene oxide electrochemical system is established to produce higher-order ethylene oxide using C₂H₄ as reactants generated from a conventional

$CO_2RR||OER$ electrolysis system (Fig. 6f). The highly-active HClO from COR initiate the oxidation of C_2H_4 to $HOCH_2CH_2Cl$ to subsequently produce ethylene oxide under alkaline condition through mixing the catholyte and anolyte output streams. This demonstration gives FE = 70% and 97% ethylene specificities at a high current of 1.0 A cm^{-2}, offering a viable prospect for higher-order products generation in series integrated systems. Interestingly, an additional heat exchanger component was added into the $CO_2RR||COR$ integrated system to avoid the problem of $KHCO_3$ precipitation on the GDE cathode, providing new ideas for the production of soda ash by the Solvay process and high-performance CO_2RR [83]. Inspired by this, additional substances can be added to the anolyte or a cascade catalytic system can be constructed to take full advantage of the strong oxidative chlorine-containing substances produced from COR to couple CO_2RR to obtain novel products.

Although the $CO_2RR||COR$ integration system has shown great promise, it should be noted that some CO_2RR catalysts such as Bi and Cu are very sensitive to halogen ions, which means that the use of NaCl electrolyte will have a significant impact on the catalyst reconstruction and electrochemical performances. The use of NaCl both as catholyte and anolyte will lead to a drastic change in the pH value of both sides during the electrolysis process. Consequently, the stability assessment should be taken into consideration for $CO_2RR||COR$ systems. Additionally, the treatment of surplus toxic Cl_2 gas is generally not considered at present. And the presence of various metal ions can also cause corrosion and clogging problems of the catalyst when electrolyzing in real seawater. Apart from the rational design of highly active cathode and anode catalysts, anti-corrosion devices and multi-functional integrated systems utilizing the oxidation properties of COR products should also be considered.

3.4. CO2RR coupled to water contaminants oxidation reaction integrated system

Over the past few years, with the rapid development of urbanization, both industrial and domestic wastewater containing a large number of inorganic and organic pollutants, such as pathogenic microorganisms, toxic metals, dangerous chemicals and textile dyes, pose a great threat to human beings and the environment [132–134]. At present, wastewater treatment methods include chemical, biological, physical, and advanced oxidation processes, among which the electrochemical method is widely used because of its environmental friendliness, easy operation, and low cost [135]. Impressively, the electrochemical coupling of CO_2RR and wastewater pollutants oxidations can simultaneously realize value-added chemicals generation converted from CO_2 and efficient purification of wastewater with reduced energetic requirements. Following this thought, the anode oxidations of nitrogenous compounds [16, 32, 136–138], dyes [134,135,139], microorganisms [140], and toxic gas [141–145] coupled to CO_2RR integrated systems will be introduced in this part. The crucial components covering electrocatalysts, electrolytes, electrolyzers, major products with corresponding maximum FEs for cathodic reaction and pollutants removal efficiency (RE) for anodic reaction are listed in Table 3. Since most of the cathode are CO- and HCOOH-producing materials with high CO_2RR performance as above-discussed, the anode counterpart within the integrated system is emphasized in this section.

3.4.1. CO2RR coupled to nitrogenous compounds oxidation reaction integrated system

Some typical nitrogenous compounds including ammonia, urea, and nitrophenol are chosen for anodic oxidation substrates. The thermodynamic potential (E^0) of urea to N_2 (UOR) and ammonia to N_2 (AnOR)

Table 3

A summary of the CO_2RR coupled to water contaminants oxidation reaction integrated system including electrocatalysts, electrolyte, electrolyzer, membrane, cell voltage, major CO_2RR products and corresponding maximum FE, organic pollutants and corresponding maximal RE for anodic reaction. (The * lable means the yield of products.).

Cathode catalyst	Catholyte	Cathode product (FE$_{max}$/%)	Anode catalyst	Anolyte	Anode product (RE$_{max}$/%)	Cell voltage [V]	Cell type (membrane)	Ref
Ag/C	5 M KOH	CO (N/A)	Pt/C	5 M KOH + 1 M NH$_3$	N$_2$ (N/A)	~2.3 V at 10 mA cm^{-2}	H-type cell (AEM)	[16]
Ag/C	5 M KOH	CO (90%)	NF	5 M KOH + 0.33 M urea	N$_2$ (N/A)	~2.5 V at 100 mA cm^{-2}	H-type cell (AEM)	[16]
CuO	0.1 M KHCO$_3$	*C$_2$H$_5$OH (41 μmol L^{-1})	Co$_3$O$_4$	0.1 M NaSO$_3$ + 10 mg/L 4-NP + appropriate PMS	RE$_{4-NP}$ (93%)	N/A	H-type cell (PEM)	[32]
Au	0.5 M KHCO$_3$	HCOOH (4.9%)	Pt/C	0.5 M KHCO$_3$ + 2 M NH$_3$	N$_2$ (N/A)	− 5.5 V at 100 mA cm^{-2}	near zero-gap cell (CEM)	[136]
Cu/Bi	0.5 M KHCO$_3$	HCOOH (~87.7%)	Ti/SnO$_2$-Sb	0.5 M KCl + 50 mg/L PNP	RE$_{PNP}$ (~97.5%)	N/A	H-type cell (PEM)	[137]
SnO$_2$/CC	0.1 M KHCO$_3$	HCOOH (33.8%)	Co$_3$O$_4$ @C	0.1 M NaSO$_3$ + 10 mg/L 4-NP + 0.5 g/L PMS	RE$_{4-NP}$ (99%)	N/A	H-type cell (PEM)	[138]
Bi	0.5 M KHCO$_3$	HCOOH (~98%)	Ti/SnO$_2$-Sb	0.5 M KCl + 500 mg/L MO	RE$_{MO}$ (100%)	N/A	flow cell (PEM)	[134]
Sn	0.1 M Na$_2$SO$_3$ + H$_2$SO$_4$ (PH=4)	*HCOOH (~8 mM)	boron doped diamond	0.1 M Na$_2$SO$_3$ + H$_2$SO$_3$ (PH=4) + 150 mg/L AO7	RE$_{AO7}$ (~100%)	N/A	H-type cell (PEM)	[135]
Co$_3$O$_4$/N-RGO	1 M KOH	CH3OH (74.8%)	Co$_3$O$_4$/N-RGO	1 M KOH + 100 mg/L MB	RE$_{MB}$ (100%)	N/A	H-type cell (PEM)	[139]
Fe SA-NC	0.5 M KHCO$_3$	*CO (34.2 mmol g$_{cat}^{-1}$ h^{-1})	bioanode	*Shewanella oneidensis* MR-1 + phosphate buffer + acetate	CO$_2$ (N/A)	~1.14 V at 1.54 mA cm^{-2}	H-type microbial electrolysis cell	[140]
Tin plate	300 mL KHCO$_3$	HCOOH (69.9%)	IrO$_2$-Ta$_2$O$_5$/ Ti	300 mL 0.3 M Na$_2$SO$_4$ + Na$_2$SO$_3$	SO$_4^{2-}$ (N/A)	N/A	H-type cell (PEM)	[141]
BiOI	1 M NaHCO$_3$	HCOOH (~91%)	NiO/NF	0.5 M NaHCO$_3$ + 0.25 M Na$_2$SO$_3$	sulfate (45%)	1.80 V at 10 mA cm^{-2}	H-type cell (PEM)	[142]
ZnO@G	1 L EMIM-BF$_4$/ H$_2$O	CO (N/A)	G/graphite carbon sheet	0.1 M EDTA-Fe^{2+} + CH$_4$ + CO$_2$ + H$_2$S	S (N/A)	1.72 V at 8.5 mA cm^{-2}	H-type cell (PEM)	[143]
CoPc	0.5 M KHCO$_3$	*CO (19.9 mg·cm^{-2}·h^{-1})	graphite felt	0.5 M KI + CH$_4$ + CO$_2$ + H$_2$S	*S (24.9 mg·cm^{-2}·h^{-1})	N/A	flow cell (PEM)	[144]
BiOCl	1 M KOH	HCOOH (~96%)	Cu$_2$O	1 M KOH + 0.1 M formaldehyde	HCOOH (~96%)	0.86 V at 100 mA cm^{-2}	MEA (BPM)	[145]

calculated from Gibbs free energy is estimated to be 0.07 and 0.06 V (vs. RHE, pH = 14), respectively, emerging as reasonably energy-saving OER-alternative reactions. Expectedly, Medvedeva et al. [16] employed these two alternative reactions coupled with CO_2RR to construct integrated systems with remarkably reduced $|U_{cell}^0|$ by 0.9–1.2 V. Notably, this team also investigated electrocarboxylation coupling (ECR) of CO_2 using organic halides as substrates in aprotic media, and found that $|U_{cell}^0|$ was reduced by up to 1.2 V in the ECR|| UOR integrated system compared to traditional H-type CO_2RR||OER electrolysis (Fig. 7a). This is mainly because the addition of halides promotes the production of highly active species, which reduce the electric potential required for CO_2 activation [146]. Notably, the overall electrochemical would deteriorate due to the Pt anode poisoning by surface absorbed N-containing intermediates. To better improve the current density to foster industrialization, Choi et al. [136] constructed the CO_2RR||AnOR integrated system by using GDE in both the cathode and anode (Fig. 7b), achieving a high current density of 100 mA cm^{-2} at − 5.5 V with small charge transmission resistance. Impressively, the H_2/CO ratio reached 4:1 when the anode electrolyte contained 2 M NH_3, paving the way to generate syngas. However, the Pt-based catalyst is still used in the anode of this system, ignoring the toxic effect of reaction intermediates on the catalyst [147].

Nitrophenol often used in synthetic materials and medicine industries is a kind of extremely toxic organic pollutant existing in wastewater, posing great harm to both human health and ecological environment [148]. In recent years, electrochemical oxidation technology has served for the effective mineralization of nitrophenol [149]. For example, CuO and Co_3O_4 have been used as cathodic and anodic catalysts for simultaneous CO_2RR to yield about 98 mmol L^{-1} CH_3OH and 41 mmol L^{-1} CH_3CH_2OH and 4-nitrophenol (4-NP) oxidation with 93% RE at − 0.8 V after 2 h (Fig. 7c). Interestingly, an advanced oxidation process is successfully introduced to generate highly oxidative $SO_4^{\bullet-}$ mediated by peroxymonosulfate in the electrolyte to mineralize 4-NP (Fig. 7d). Besides, comparison studies about the effect of different anode electrolytes of Na_2SO_4, NaCl, and $NaHCO_3$ on RE of 4-NP showed that the OH$^-$ generated in the presence of $NaHCO_3$ would react with the active substances generated by AOP to reduce the RE [32]. A similar integrated system is also constructed by Zhu et al. [138] to gain 99% RE for 4-NP and a FE_{HCOOH} = 24.1% at − 1.3 V using amorphous carbon-modified Co_3O_4 and SnO_2 sheets as anode and cathode, respectively. In addition, the overall performance of simultaneous organic pollutants removal and valuable chemical production from CO_2RR can be regulated by electrochemical parameters to further meet the requirements of industrialization [137].

The high-performance electrocatalysts ensure efficient functionalization of the integrated system for CO_2 conversion and nitrogenous compounds oxidations. Nevertheless, the fact that metal oxides cathode (such as CuO and SnO_2) are easily reduced at reduction potentials is usually overlooked. At the same time, the surface poisoning of the anodic electrocatalyst surface by N-containing intermediates will result in a drop of its electrochemical activity and stability. Consequently, electrocatalysts are still the key point for sustainability at both ends of the integrated system. This system still confronted with great challenges associated with membrane permeability by ions and membrane blockage by N-containing species.

3.4.2. CO_2RR coupled to dyes oxidation reaction integrated systems

Typical azo pollutants from dye wastewater including methyl orange (MO), acid orange 7 (AO7), and methylene blue (MB), have also been used for paired electrochemical reactions with CO_2RR. Wang et al. [134] compared the impact of KCl and $KHCO_3$ electrolytes on the RE of MO by constructing a CO_2RR-coupled MO oxidation system using a Bi cathode and Ti/SnO_2-Sb anode. As shown in Fig. 7e, 100% RE of MO was gained in the KCl electrolyte, probably due to the strong oxidation of highly active chlorine species. Furthermore, an economic evaluation of AO7 treatment using boron-doped diamond as an anode catalyst shows that

the operation cost is between 13 and 35 € m^{-3} with great advantages over the Fenton and ozonation methods, further promoting the establishment of the integrated system of dye pollutants oxidation and CO_2RR towards commercialization [135]. Since the high price of boron-doped diamond electrocatalysts becomes an obstacle [150], more efforts are still needed for the design of the anode catalyst. To this end, a bifunctional catalyst of Co_3O_4 on N-doped reduced GO was recently reported to accomplish a 74.8% FE of CO_2-to-CH_3OH and 100% RE of MB at − 0.7 V in a combination of CO_2RR and MB oxidation co-electrolysis. This is because the sheet network structure of the material offers a large specific surface area and the N-doped reduced GO participates in the modification of Co atoms to provide more active centers [139].

In spite of great prospects, the overall reaction process and reaction intermediates still need to be systematically studied, because multiple ions in these dyes may have certain effects on the membrane, electrocatalyst, and the whole system. Particularly, the dyes at the anode are usually degraded under the action of strong oxidizing species generated, which is also detrimental to the IEM stability. Especially, the membrane deterioration becomes more severe with the accumulation of oxidative radicals, as it often takes a relatively long time to fully oxidize dyes.

3.4.3. CO_2RR coupled to microorganisms oxidation reaction integrated systems

Until now, bioelectrochemical systems have been developed in wastewater treatment by using electrochemically active bacteria to oxidize organic materials and the parasitically generated electrons transferred to cathode for specific reduction reactions, promoting the conversion of chemical energy to electrical energy [151]. Conceivably, an integrated device composed of bioelectrochemical systems plays an important role in reducing the energy input for CO_2RR. Li et al. [140] successfully integrated CO_2RR to CO on Fe single atom cathode with *Shewanella oneidensis* bacteria as bioanode. With the help of an external microbial fuel cell delivering a power density of up to 0.46 W m^{-2}, this device can achieve a CO production rate of about 34 mmol g^{-1} h^{-1} (Fig. 7f and g). Due to the difficulty in the compatibility of inorganic-organic hybrids, studies on the successful construction of CO_2RR coupled microorganisms oxidation reaction integrated systems are very limited. The research on microbial fuel cells can provide a reference for further investigations on coupled systems.

The anodic microbial metabolic rate is too low to output the required electrical energy for cathodic CO_2RR with a high energetical barrier, so an external electrical source is generally needed. It is necessary to extend the potential of powering CO_2RR entirely with energy recovered and carbon source from bio-driven wastewater treatment in future studies. It should be noted that organic matter and suitable electrolyte microenvironment are needed to be strictly selected to ensure the electrochemically active bacteria triggered oxidation reactions. Meanwhile, the active microorganisms or their intermediates after inactivation in the electrolyte will also cause the degradation of membranes and electrodes. Since the high oxidation potential and the oxidative species produced by electrolysis can also directly inactivate microorganisms, the mechanism study of anodic oxidations is more complicated. That is to say, fundamental studies obtaining mechanistic information on the integrated system of CO_2RR coupled microorganisms oxidation reaction should be further strengthened in the near future.

3.4.4. CO_2RR coupled to toxic gas oxidation reaction integrated systems

With the rapid development of industrialization, air pollution is becoming more and more serious to affect human health. In particular, living with some toxic gases, such as SO_2, H_2S, and formaldehyde, may cause cancer and death through long-term exposure [152]. Regarding the relatively high solubility of these gases in aqueous solution, oxidations of these gases dissolved matters are also a possible option to integrate with CO_2RR with greater advantages over OER. In this scenario, the oxidation reactions in the Na_2SO_3 and H_2S electrolyte used as an alternative anode reaction for CO_2RR can reduce the cell voltage and
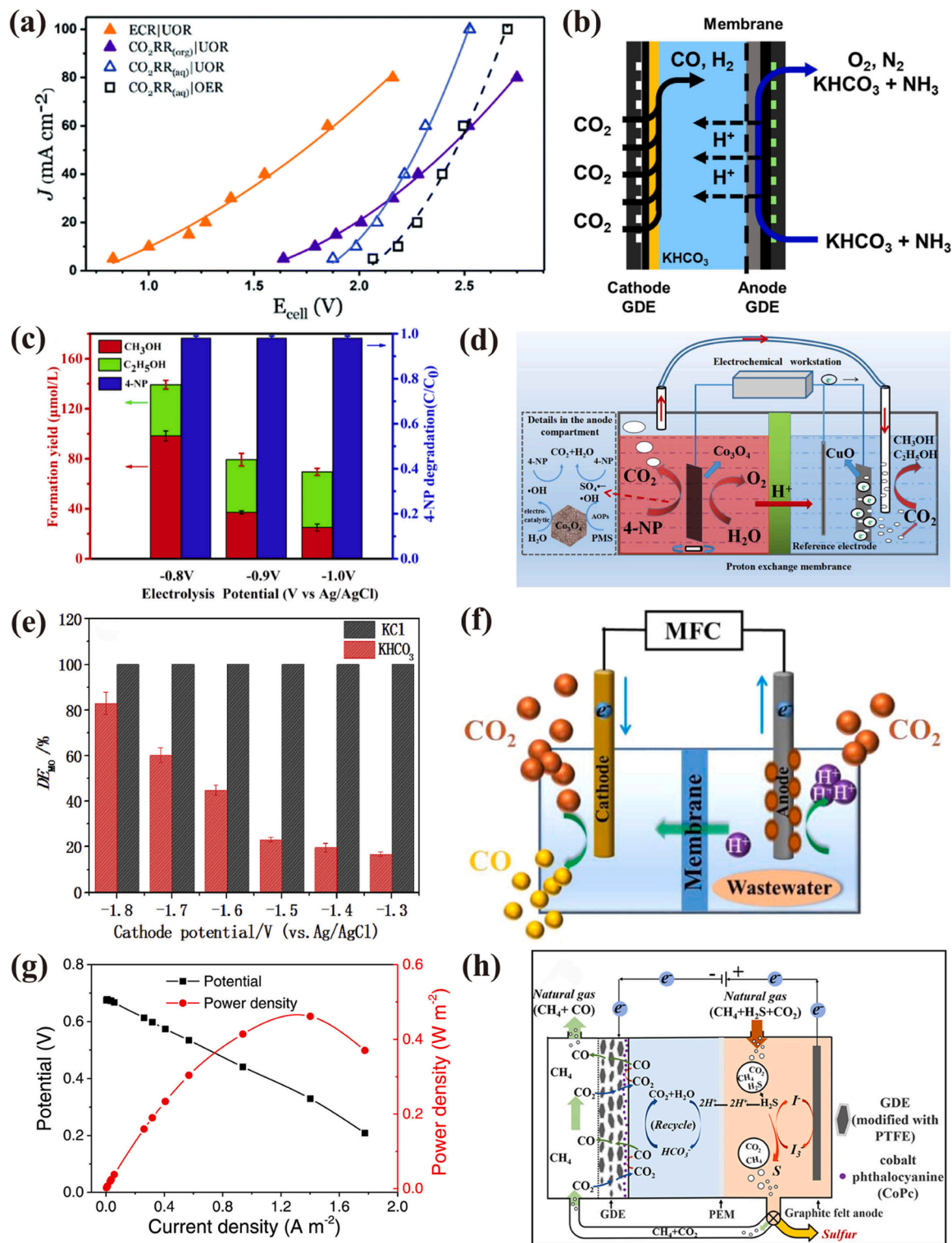
Fig. 7. (a) The total current density as a function of cell voltages for different integrated systems [16]. (b) The near zero-gap cell using GDE in both the cathode and anode for CO$_2$RR||AnOR integrated system [136].(c) FEs of methanol and ethanol from CO$_2$RR and RE of 4-NP and (d) possible mechanism for 4-NP mineralization and methanol and ethanol generation within integrated systems [32]. (e) The REs of MO on Ti/SnO$_2$-Sb anode at different cathode potentials using KCl and KHCO$_3$ electrolyte [134]. (f) Schematic illustration of a bioelectrochemical system powered by an external microbial fuel cell equipped with CO$_2$RR cathode and bacteria bioanode and (g) corresponding polarization curve and power density of this device [140]. (h) Operation principle diagram of the high yield of. A two-flow electrolyzer using cathode GDE and an I$^-$/I$_3^-$ cyclic oxidation for CO formation and S recovery [144].

enhance the EE of the overall electrolysis system compared to the $CO_2RR||OER$ system [141,142]. Moreover, additional redox couples (EDTA-Fe^{2+}/EDTA-Fe^{3+}) in the anode are sometimes introduced into the integrated system to accelerate the reactions [143]. Despite the improved electrochemical performance, the effect of the introduced ions on the membrane and catalyst becomes a crucial point to be considered. Particularly, the deposition of anode product S will also cause the anode catalyst passivation, so the system has strict requirements for electrolyzer. Interestingly, to avoid anode passivation, a two-flow electrolyzer using cathode GDE and an I^-/I_3^- cyclic oxidation system has been constructed (Fig. 7h). A natural gas mixture of CH_4, CO_2, and H_2S is first injected into the anodic chamber where H_2S is oxidized to the suspended S with further separation. Subsequently, the unreacted CH_4/CO_2 gases passed through the GDE to participate in CO_2RR for CO generation. As a result, over 95% CO selectivity and 24.94 mg·cm^{-2}·h^{-1} S yielding at 50 mA cm^{-2} current density is achieved. To avoid the degradation of CO_2RR performance due to proton consumption and insufficient supply of CO_2 and H^+ at high current density, phenol-modified and PTFE-modified GDEs were also used to provide additional protons and enhance CO_2 transport efficiency [144]. This work not only effectively converts H_2S gas but also broadens the path for efficient CO_2RR under a large current. Toxic gases must be dissolved in the electrolyte prior to the electrocatalytic oxidation reactions. However, subsequent collection and treatment of undissolved toxic gases become a big problem due to solubility limitation. Also, insoluble oxidation products such as sulfur will be produced. This requires an effective exhaust gas treatment and product collection device for sustainability.

Formaldehyde is a key precursor in the manufacture of resins, rubbers, paints, medicine and pesticide, which also results in the discharge pollution of formaldehyde-containing wastewater [153]. Meanwhile, formaldehyde oxidation reaction (FOR), as a method of producing HCOOH mediated by a one-electron transfer process with a low standard thermodynamic potential (0.14 V vs. RHE) than OER, also has great advantages in coupling with CO_2RR. Li et al. [145] successfully coupled $CO_2RR||FOR$ system using BiOCl cathode and Cu_2O anode separated by BPM to avoid short circuits and electrolyte leakage caused by anode catalyst penetration. Furthermore, the unique zero-gap configuration of MEA system achieved an average of 192% FE for the co-production of HCOOH, which will provide a new idea for the efficient electrosynthesis of high-value chemicals. Owing to the instability of formaldehyde, it is extremely difficult to construct a stable $CO_2RR||FOR$ coupling system. Given formaldehyde is highly toxic, long-term exposure to formaldehyde should not be allowed during the experiment to avoid sensitization.

Although the integration system of CO_2RR coupled to water contaminants oxidations has shown certain advantages in low energy input and wastewater purification, its further development is hindered by the fact that the anode products are mostly CO_2 and N_2 of no economic value. In addition, the presence of other ions in the wastewater, nitrogen-containing intermediates in the reaction process and the oxidation product S can also cause deterioration of the catalyst and membrane. Laboratory experiments usually use simple simulated wastewater, but the composition of wastewater is often more complex in practical applications. The substantial effort to advance this integration system of CO_2RR coupled to water contaminants oxidations into practical applications is important but also extremely challenging.

3.5. CO_2RR coupled to chemicals electrosynthesis integrated system

Electrochemical synthesis of a variety of organic intermediates, especially pharmaceutical intermediates, are economically attractive for the extending applications of CO_2RR precipitated integrated systems [154–156]. Liang et al. [154] and Zhu et al. [155] have successfully paired CO_2RR with octylamine and tetrahydroisoquinoline oxidations, respectively, with advantageous lowered cell voltages to decrease energy consumption compared with $CO_2RR||OER$ system. More importantly, the octylamine and tetrahydroisoquinoline can be high-selectively (FE > 98%) electrooxidized to value-added pharmaceutical intermediate octanenitrile and dihydroisoquinoline at the anode chamber of the established integrated systems. Similar to the aforementioned cases, HCOOH-producing Bi and Sn based nanostructured electrocatalysts were used in the cathodic side. Moreover, transition metal based single atom or molecular nanostructures are well-known CO_2-to-CO electrocatalysts with impressive selectivity, which also present outstanding oxidative capabilities towards organics. Exhilaratingly, using single Ni atoms grown on N-doped CNTs (NiSA/CNT) as bifunctional electrocatalysts separated by BPM, the two-electrode electrolysis achieved the best CO FE of 99.3% and benzonitrile FE of 98% for cathodic CO_2RR and anodic benzylamine oxidation, respectively [156]. As shown in Fig. 8a, the current density during electrolysis is stabilized for 200 h without deterioration at the electrolyte refresh mode. Similar integrated system was also developed for selective CO_2-to-CO conversion coupled to oxidative levodopa polymerization [157]. Unfortunately, the yields of these high-value chemicals are limited by the low current densities. Most of the current integrated systems are constructed through a simple combination of CO_2RR and anodic oxidative reactions mainly for the purpose of studying the redox reactions in two individual chambers. This configuration can facilitate the products collection and also prevent direct contact of different substances produced by two electrodes from interfering with each other. On second thought, some research efforts have been attempted in integrating the intermediates or products during redox reactions with a subsequent reaction in a membrane-free single cell for the electrosynthesis of more complex functional chemicals. As a proof-of-concept, Zhong et al. [158] designed a coupling device using a single-chamber cell that successfully combined CO_2 with Br_2 to produce the specific oxygen-containing compound 2-bromo-ethanol with FE = 40% and a partial current density of − 19 mA cm^{-2} at about − 1.0 V RHE. Compared with the conventional CO_2RR products ($1300 per ton for CO and $800 per ton for C_2H_4), 2- bromo-ethanol as an important feedstock in chemical and pharmaceutical has much higher value ($21 000 per ton), which provides a new idea for generating products with higher value from CO_2RR. Notably, KBr is added into the $KHCO_3$ electrolyte for thermodynamically preferred Br_2 generation instead of O_2 from OER. The control experiments conducted in two types of chambers propose that the bromination is ascribed to Br_2 other than Br^- (Fig. 8b and c). Inspiredly, dimethyl carbonate was recently produced for the first time in a single-chamber cell via an innovative continuous oxidation process using 10%Pd/C cocatalysts dispersed and CO_2-saturated 0.1 M KBr-CH_3OH electrolyte [159]. As illustrated in Fig. 8d, CO and CH_3O^- are generated on Ni single atoms cathode while Br_2 is produced by Br^- oxidation on carbon cloth to chemically oxidize dispersed Pd to Pd^{2+}. Subsequently, dimethyl carbonate (DMC) is formed by the chemical oxidation reaction of CO and CH_3O^- species over Pd^{2+}, along with Pd^{2+} chemically reduction to Pd. Cheeringly, the FE for this environmental-benign dimethyl carbonate formation can reach 80% at 12 mA cm^{-2} and has outperformed previously reported values for DMC electrosynthesis (Fig. 8e). This synthetic system avoids the thermodynamic limitations and reactants hazards of traditional DMC synthesis, and also broadens the horizon for electrochemical synthesis of polymer building blocks through an innovative CO_2 utilization strategy.

Overall, electrochemical synthesis of refinery chemicals by the virtue of specifically designed integrated system opens up a new horizon in CO_2 utilization. Future directions include developing value-added reaction pathways, synthesizing highly active and durable catalysts, and designing high-current-density devices. With further efforts to improve the product yields, effective products separation and purification technology is a necessary means to obtain high-quality fine chemicals in the future.
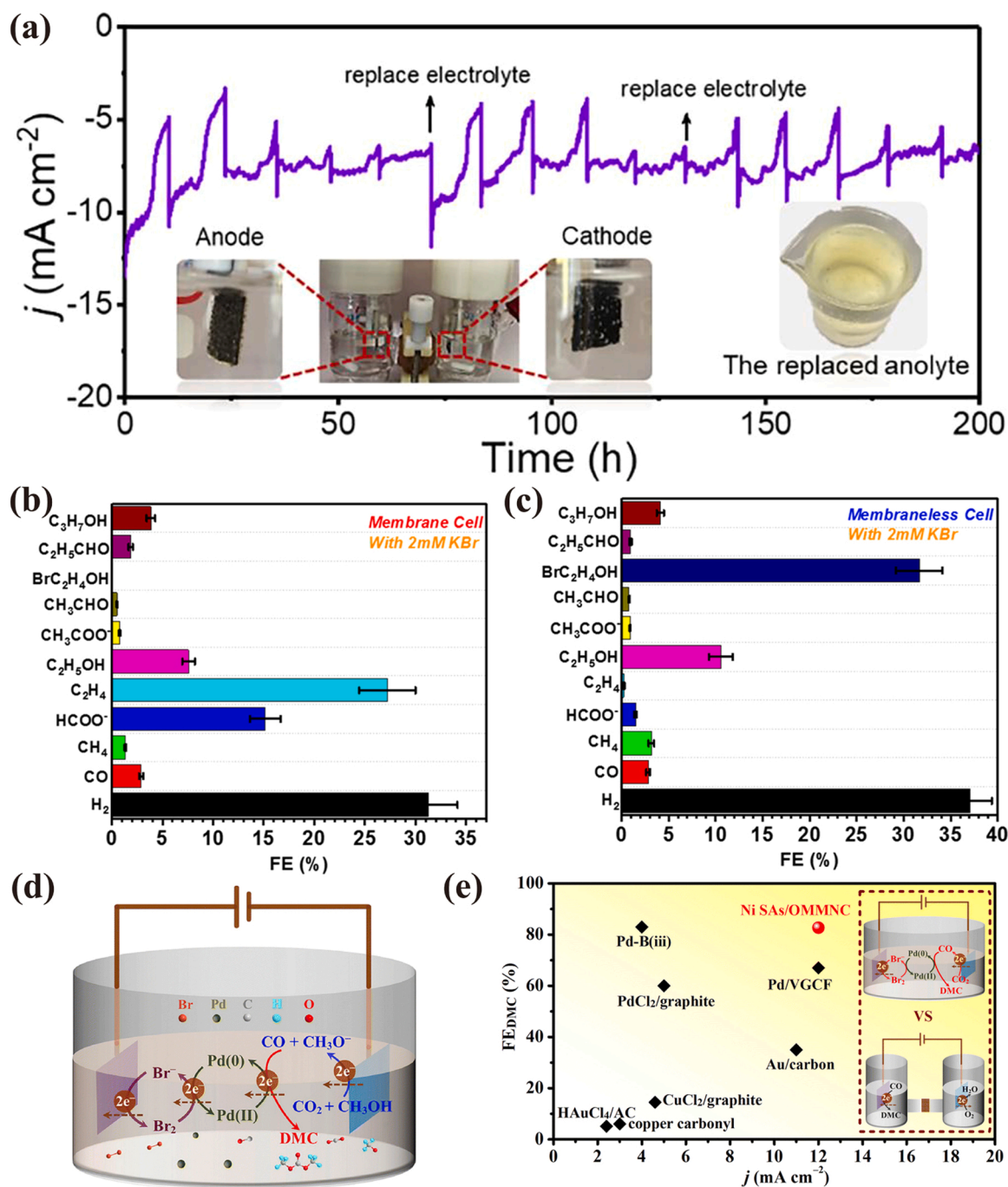
Fig. 8. (a) Stability test for 200 h at 3.0 V for NiSA/CNT cathode [156]. (b) and (c) CO_2RR performance in membrane or membraneless cell with or without KBr in electrolyte at − 0.96 V RHE [158]. (d) Schematic illustration for electrosynthesis of DMC from CO_2 and (e) Performance comparisons of DMC formation from CO_2 between convergent paired electrosynthesis and previous reports [159].

4. Conclusions and perspectives

Electrocatalytic CO_2RR technology offers a promising avenue to address global environmental and energy issues. To date, various anodic reactions mainly including the oxidations of alcohols, biomass, chlorine and water contaminants as well as chemicals electrosynthesis have been reported as OER-alternative pairing reactions to show bright prospects with economic feasibility toward CO_2RR technology. However, current research on such integrated systems is still at its early stages and the main concern is on the cathode side. To better understand the potential benefits and advantages over conventional $CO_2RR||OER$ electrolysis, we have systematically reviewed the research progress in recent five years about various electrolysis systems of OER-alternative anode reactions coupled to CO_2RR. The influences of the contributors mainly concerning the electrocatalyst, electrolyte and electrolyzer on the reaction performance of the overall integrated setup have been emphasized. Admittedly, opportunities and challenges coexist. Although these pioneering studies have shown great promise for the development of innovative paired systems, several key issues still need to be further solved in the future.

(1) High-performance electrocatalysts are still one of the most important concerns within the integrated system. The performance of the cathodic and anodic catalysts predominantly

determines the selectivity of specific products and the stability of the system, especially under large current densities. To make the whole system show better performance, it is necessary to have a clear recognition of the structure-catalytic activity relationship concerning materials structure, catalytic mechanism, and the underlying degradation mechanism of electrode catalysts, especially for the anode catalysts which are less studied at present. Rather than unilaterally focusing on the study of C1-targeting CO_2RR electrocatalysts, it is expected to give impetus to progress in high-performance electrocatalysts for both cathode and anode with large current density, high product selectivity in a wide potential range with stable performance, pushing the integrated systems closer to industrialization.

(2) The selection of electrolytes is also a non-negligible point. For cathodic side, the electrolyte induced pH variations during the reaction process may affect the solubility of CO_2. For the anodic side, the electrolytes with multiple components maybe bring some unwanted side reactions and damage to the membranes. Control experiments concerning the composition and concentration of electrolytes are necessary to be conducted to determine the optimal electrolyte for the system. In this regard, the BPM, allowing the use of different electrolytes at the cathode and anode, provides technical support to mitigate the electrolyte mismatch problem. Moreover, electrolyte ions penetration and diffusion between two chambers will be controlled with further optimization of product selectivity and catalyst stability. Therefore, an appropriate combination of the catholyte and anolyte will be advantageously helpful for the establishment of a more excellent CO_2RR coupling integrated system in the future. From the viewpoint of economics, the integrated system should be allowed to operate under the unprecedentedly high concentration substrates, thereby increasing the yield of high-value products.

(3) The electrolyzer design is also the key to establishing energy-efficient integrated systems. The next step should compare different types of electrolyzers equipped with various membranes and electrodes to enhance the overall EE for energy saving. Most of the current research are based on traditional H-type cells or flow cells, which fall behind in meeting the industrialization requirements. Therefore, exploring tandem electrolyzers or rational cell configurations referring to the high-performance conventional CO_2RR||OER systems will inject impetus into the industrialization of the integrated system and give new ideas for valuable refinery chemicals production. More importantly, the crossover and interspersion of the generated species from cathodic and anodic side functionalized by different membranes also result in inaccurate calculation of FE, EE and product yields. Thus, meticulous quantification and qualification of products for co-electrolysis is strongly suggested.

(4) The economic analysis of the paired system and the evaluation criteria of anodic oxidation reactions also need to be further unified. Thermodynamical preference is usually the first choice for OER-alternative reactions for CO_2RR. Uncovering more anodic reactions that can produce high-value chemicals would be of great economic interest to pair CO_2RR. However, economic assessments remain questionable due to diverse product and intermediate combinations and complex process design variability for reactants mixture, desirable products separation, collection and purification. Accordingly, an analysis model is preferentially addressed to evaluate the economic feasibility of the system as well as provide an evaluation reference for both sides.

(5) A complete electrolytic system including initial CO_2 capture, anode raw material acquisition, and subsequent processing of cathodic and anodic products should also be emphasized. Especially, more innovative anodic reactions for valuable chemicals and fuels production and the assistive technologies such as light, thermal, pulse, and ultrasonication to further enhance the reaction rate and EE of CO_2RR coupled integration system should be further developed.

In conclusion, with the rapid development of renewable energy and the continuous establishment of innovative CO_2RR participated integration systems, it is believed that in the near future, a green and efficient carbon conversion integrated system that is economically feasible and meets the requirements of industrialization will be truly established.

Declaration of Competing Interest

The authors declare that they have no known competing financial interests or personal relationships that could have appeared to influence the work reported in this paper.

Data availability

No data was used for the research described in the article.

Acknowledgements

Appendix A. Supporting information

Supplementary data associated with this article can be found in the online version at doi:10.1016/j.apcatb.2023.123291.

References

[1] S.C. Peter, Reduction of CO_2 to chemicals and fuels: a solution to global warming and energy crisis, ACS Energy Lett. 3 (2018) 1557–1561.
[2] L.K. Putri, B.J. Ng, W.J. Ong, S.P. Chai, A.R. Mohamed, Toward excellence in photocathode engineering for photoelectrochemical CO_2 reduction: design rationales and current progress, Adv. Energy Mater. 12 (2022) 2201093.
[3] X. Zhang, Z. Zhang, H. Li, R. Gao, M. Xiao, J. Zhu, M. Feng, Z. Chen, Insight into heterogeneous electrocatalyst design understanding for the reduction of carbon dioxide, Adv. Energy Mater. 12 (2022) 2201461.
[4] C.R. Schwalm, S. Glendon, P.B. Duffy, RCP8.5 tracks cumulative CO_2 emissions, Ind. Crops Prod. 117 (2020) 19656–19657.
[5] W. Dong, H. Xiao, Y. Jia, L. Chen, H. Geng, S.U.H. Bakhtiar, Q. Fu, Y. Guo, Engineering the defects and microstructures in ferroelectrics for enhanced/novel properties: An emerging way to cope with energy crisis and environmental pollution, Adv. Sci. 9 (2022) 2105368.
[6] L. Atwoli, A.H. Baqui, T. Benfield, R. Bosurgi, F. Godlee, S. Hancocks, R. Horton, L. Laybourn-Langton, C.A. Monteiro, I. Norman, K. Patrick, N. Praities, M.G. M. Olde Rikkert, E.J. Rubin, P. Sahni, R. Smith, N. Talley, S. Turale, D. Vázquez, Call for emergency action to limit global temperature increases, restore biodiversity, and protect health, Nutr. Rev. 79 (2021) 1183–1185.
[7] Z. Xu, C. Peng, G. Zheng, Coupling value-added anodic reactions with electrocatalytic CO_2 reduction, Chem. Eur. J. 29 (2023), e202203147.
[8] G. Wang, J. Chen, Y. Ding, P. Cai, L. Yi, L. Li, C. Tu, Y. Hou, Z. Wen, L. Dai, Electrocatalysis for CO_2 conversion: from fundamentals to value-added products, Chem. Soc. Rev. 50 (2021) 4993–5061.
[9] S. Wang, Z. Qian, Q. Huang, Y. Tan, F. Lv, L. Zeng, C. Shang, K. Wang, G. Wang, Y. Mao, Y. Wang, Q. Zhang, L. Gu, S. Guo, Industrial-level CO_2 electroreduction using solid-electrolyte devices enabled by high-loading nickel atomic site catalysts, Adv. Energy Mater. 12 (2022) 2201278.
[10] X. Jiang, L. Lin, Y. Rong, R. Li, Q. Jiang, Y. Yang, D. Gao, Boosting CO_2 electroreduction to formate via bismuth oxide clusters, Nano Res. (2022).
[11] L.K. Gao, X. Cui, C.D. Sewell, J. Li, Z.Q. Lin, Recent advances in activating surface reconstruction for high-efficiency oxygen evolution reaction, Chem. Soc. Rev. 50 (2021) 8428–8469.
[12] J. Na, B. Seo, J. Kim, C.W. Lee, H. Lee, Y.J. Hwang, B.K. Min, D.K. Lee, H.S. Oh, U. Lee, General technoeconomic analysis for electrochemical coproduction coupling carbon dioxide reduction with organic oxidation, Nat. Commun. 10 (2019) 5193.
[13] X. Zhao, L. Du, B. You, Y. Sun, Integrated design for electrocatalytic carbon dioxide reduction, Catal. Sci. Technol. 10 (2020) 2711–2720.
[14] G. Bharath, A. Hai, K. Rambabu, P. Kallem, M.A. Haija, F. Banat, J. Theerthagiri, M.Y. Choi, Fabrication of Pd/MnFe$_2$O$_4$ bifunctional 2-D nanosheets to enhance the yield of HCOOH from CO_2 cathodic reduction paired with anodic oxidation to CH_3OH, Fuel 311 (2022), 122619.

[15] Y. Zhou, Z. Wang, W. Fang, R. Qi, Z. Wang, C. Xia, K. Lei, B. You, X. Yang, Y. Liu, W. Guo, Y. Su, S. Ding, B.Y. Xia, Modulating O–H activation of methanol oxidation on nickel-organic frameworks for overall CO₂ electrolysis, ACS Catal. 13 (2023) 2039–2046.

[16] X.V. Medvedeva, J.J. Medvedev, S.W. Tatarchuk, R.M. Choueiri, A. Klinkova, Sustainable at both ends: electrochemical CO₂ utilization paired with electrochemical treatment of nitrogenous waste, Green. Chem. 22 (2020) 4456–4462.

[17] C. Hu, Y. Zhang, A. Hu, Y. Wang, X. Wei, K. Shen, L. Chen, Y. Li, Near- and long-range electronic modulation of single metal sites to boost CO₂ electrocatalytic reduction, Adv. Mater. 35 (2023), e2209298.

[18] F. Ye, S. Zhang, Q. Cheng, Y. Long, D. Liu, R. Paul, Y. Fang, Y. Su, L. Qu, L. Dai, C. Hu, The role of oxygen-vacancy in bifunctional indium oxyhydroxide catalysts for electrochemical coupling of biomass valorization with CO₂ conversion, Nat. Commun. 14 (2023) 2040.

[19] S. Hussain, E. Aneggi, D. Goi, Catalytic activity of metals in heterogeneous Fenton-like oxidation of wastewater contaminants: a review, Environ. Chem. Lett. 19 (2021) 2405–2424.

[20] X. Zhang, Y. Wang, M. Gu, M. Wang, Z. Zhang, W. Pan, Z. Jiang, H. Zheng, M. Lucero, H. Wang, G.E. Sterbinsky, Q. Ma, Y.G. Wang, Z. Feng, J. Li, H. Dai, Y. Liang, Molecular engineering of dispersed nickel phthalocyanines on carbon nanotubes for selective CO₂ reduction, Nat. Energy 5 (2020) 684–692.

[21] A. Löwe, M. Schmidt, F. Bienen, D. Kopljar, N. Wagner, E. Klemm, Optimizing reaction conditions and gas diffusion electrodes applied in the CO₂ reduction reaction to formate to reach current densities up to 1.8 A cm⁻², ACS Sustain. Chem. Eng. 9 (2021) 4213–4223.

[22] S. Hu, H. Li, X. Dong, Z. Cao, B. Pang, L. Zhang, W. Yu, J. Xiao, X. Zhu, W. Yang, Rational design of CO₂ electroreduction cathode via in situ electrochemical phase transition, J. Energy Chem. 66 (2022) 603–611.

[23] D. Li, J. Yang, J. Lian, J. Yan, S. Liu, Recent advances in paired electrolysis coupling CO₂ reduction with alternative oxidation reactions, J. Energy Chem. 77 (2023) 406–419.

[24] W. Zhong, W. Huang, S. Ruan, Q. Zhang, Y. Wang, S. Xie, Electrocatalytic reduction of CO₂ coupled with organic conversion to selectively synthesize high-value chemicals, Chem. Eur. J 29 (2023), e202203228.

[25] R. Lin, J. Guo, X. Li, P. Patel, A. Seifitokaldani, Electrochemical reactors for CO₂ conversion, Catalysts 10 (2020) 473.

[26] X.H. Zhong, S.J. Liang, T.T. Yang, G.C. Zeng, Z.Q. Zhong, H. Deng, L. Zhang, X. L. Sun, Sn dopants with synergistic oxygen vacancies boost CO₂ electroreduction on CuO nanosheets to CO at low overpotential, ACS Nano 16 (2022) 19210–19219.

[27] K. Liu, W.A. Smith, T. Burdyny, Introductory guide to assembling and operating gas diffusion electrodes for electrochemical CO₂ reduction, ACS Energy Lett. 4 (2019) 639–643.

[28] M. Abdinejad, A. Seifitokaldani, C. Dao, E.H. Sargent, Xa Zhang, H.B. Kraatz, Enhanced electrochemical reduction of CO₂ catalyzed by cobalt and iron amino porphyrin complexes, ACS Appl. Energy Mater. 2 (2019) 1330–1335.

[29] F. Proietto, I. Patel, A. Galia, O. Scialdone, Electrochemical conversion of CO₂ to formic acid using a Sn based electrode: a critical review on the state-of-the-art technologies and their potential, Electrochim. Acta 389 (2021), 138753.

[30] C.B. Chen, Y.F. Li, P.D. Yang, Address the "alkalinity problem'' in CO₂ electrolysis with catalyst design and translation, Joule 5 (2021) 737–742.

[31] R. Ge, L.Y. Dong, X. Hu, Y.T. Wu, L. He, G.P. Hao, A.H. Lu, Intensified coupled electrolysis of CO₂ and brine over electrocatalysts with ordered mesoporous transport channels, Chem. Eng. J. 438 (2022).

[32] J.P. Zou, Y. Chen, S.S. Liu, Q.J. Xing, W.H. Dong, X.B. Luo, W.L. Dai, X. Xiao, J. M. Luo, J. Crittenden, Electrochemical oxidation and advanced oxidation processes using a 3D hexagonal Co₃O₄ array anode for 4-nitrophenol decomposition coupled with simultaneous CO₂ conversion to liquid fuels via a flower-like CuO cathode, Water Res 150 (2019) 330–339.

[33] Y. Mi, Y. Qiu, Y. Liu, X. Peng, M. Hu, S. Zhao, H. Cao, L. Zhuo, H. Li, J. Ren, X. Liu, J. Luo, Cobalt-iron oxide nanosheets for high-efficiency solar-driven CO₂-H₂O coupling electrocatalytic reactions, Adv. Funct. Mater. 30 (2020) 2003438.

[34] B. Wulan, L. Zhao, D. Tan, X. Cao, J. Ma, J. Zhang, Electrochemically driven interfacial transformation for high-performing solar-to-fuel electrocatalytic conversion, Adv. Energy Mater. 12 (2022) 2103960.

[35] A. Gawel, T. Jaster, D. Siegmund, J. Holzmann, H. Lohmann, E. Klemm, U.-P. Apfel, Electrochemical CO₂ reduction-the macroscopic world of electrode design, reactor concepts & economic aspects, iScience 25 (2022), 104011.

[36] J.J. Lv, R. Yin, L. Zhou, J. Li, R. Kikas, T. Xu, Z.J. Wang, H. Jin, X. Wang, S. Wang, Microenvironment engineering for the electrocatalytic CO₂ reduction reaction, Angew. Chem. Int. Ed. 61 (2022), e202207252.

[37] U.O. Nwabara, E.R. Cofell, S. Verma, E. Negro, P.J.A. Kenis, Durable cathodes and electrolyzers for the efficient aqueous electrochemical reduction of CO₂, ChemSusChem 13 (2020) 855–875.

[38] W.R. Leow, Y. Lum, A. Ozden, Y. Wang, D.H. Nam, B. Chen, J. Wicks, T. T. Zhuang, F. Li, D. Sinton, E.H. Sargent, Chloride-mediated selective electrosynthesis of ethylene and propylene oxides at high current density, Science 368 (2020) 1228–1233.

[39] R. Ge, X. Hu, L.Y. Dong, D. Li, G.P. Hao, Electrochemical coupling between cathodic carbon dioxide reduction and anodic oxidation synthesis, Chem. Ind. Eng. Prog. (2021) 5132–5144.

[40] D.A. Salvatore, C.M. Gabardo, A. Reyes, C.P. O'Brien, S. Holdcroft, P. Pintauro, B. Bahar, M. Hickner, C. Bae, D. Sinton, E.H. Sargent, C.P. Berlinguette, Designing anion exchange membranes for CO₂ electrolysers, Nat. Energy 6 (2021) 339–348.

[41] F. Habibzadeh, P. Mardle, N. Zhao, H.D. Riley, D.A. Salvatore, C.P. Berlinguette, S. Holdcroft, Z. Shi, Ion exchange membranes in electrochemical CO₂ reduction processes, Electrochem. Energy Rev. 6 (2023).

[42] Z. Zhang, Y. Xie, Y. Wang, What matters in the emerging application of CO₂ electrolysis, Curr. Opin. Electrochem. 34 (2022), 101012.

[43] W. Lai, Y. Qiao, J. Zhang, Z. Lin, H. Huang, Design strategies for markedly enhancing energy efficiency in the electrocatalytic CO₂ reduction reaction, Energy Environ. Sci. 15 (2022) 3603–3629.

[44] Y. Quan, J. Zhu, G. Zheng, Electrocatalytic reactions for converting CO₂ to value-added products, Small Sci. 1 (2021) 2100043.

[45] K. Xie, A. Ozden, R.K. Miao, Y. Li, D. Sinton, E.H. Sargent, Eliminating the need for anodic gas separation in CO₂ electroreduction systems via liquid-to-liquid anodic upgrading, Nat. Commun. 13 (2022) 3070.

[46] M.G. Kibria, J.P. Edwards, C.M. Gabardo, C.T. Dinh, A. Seifitokaldani, D. Sinton, E.H. Sargent, Electrochemical CO₂ reduction into chemical feedstocks: from mechanistic electrocatalysis models to system design, Adv. Mater. 31 (2019) 1807166.

[47] M. Jouny, W. Luc, F. Jiao, General Techno-economic analysis of CO₂ electrolysis systems, Ind. Eng. Chem. Res. 57 (2018) 2165–2177.

[48] C. Palmer, F. Saadi, E.W. McFarland, Technoeconomics of commodity chemical production using sunlight, ACS Sustain. Chem. Eng. 6 (2018) 7003–7009.

[49] S. Verma, S. Lu, P.J.A. Kenis, Co-electrolysis of CO₂ and glycerol as a pathway to carbon chemicals with improved technoeconomics due to low electricity consumption, Nat. Energy 4 (2019) 466–474.

[50] P. Zhu, H. Wang, High-purity and high-concentration liquid fuels through CO₂ electroreduction, Nat. Catal. 4 (2021) 943–951.

[51] S.A. Hawks, V.M. Ehlinger, T. Moore, E.B. Duoss, V.A. Beck, A.Z. Weber, S. E. Baker, Analyzing Production rate and carbon utilization trade-offs in CO₂RR electrolyzers, ACS Energy Lett. 7 (2022) 2685–2693.

[52] O.S. Bushuyev, P. De Luna, C.T. Dinh, L. Tao, G. Saur, J. van de Lagemaat, S. O. Kelley, E.H. Sargent, What should we make with CO₂ and how can we make it? Joule 2 (2018) 825–832.

[53] C.S. Cao, D.D. Ma, J.C. Jia, Q. Xu, X.T. Wu, Q.L. Zhu, Divergent Paths, Same goal: a pair-electrosynthesis tactic for cost-efficient and exclusive formate production by metal-organic-framework-derived 2D electrocatalysts, Adv. Mater. 33 (2021) 2008631.

[54] Y.C. He, D.D. Ma, S.H. Zhou, M. Zhang, J.J. Tian, Q.L. Zhu, Integrated 3D open network of interconnected bismuthene arrays for energy-efficient and electrosynthesis-assisted electrocatalytic CO₂ reduction, Small 18 (2022) 2105246.

[55] Y. Li, C.Z. Huo, H.J. Wang, Z.X. Ye, P.P. Luo, X.X. Cao, T.B. Lu, Coupling CO₂ reduction with CH₃OH oxidation for efficient electrosynthesis of formate on hierarchical bifunctional CuSn alloy, Nano Energy 98 (2022), 107277.

[56] Z. Li, Y. Gao, X. Meng, B. Sun, K. Song, Z. Wang, Y. Liu, Z. Zheng, P. Wang, Y. Dai, H. Cheng, B. Huang, In-situ-derived self-selective electrocatalysts for solar formate production from simultaneous CO₂ reduction and methanol oxidation, Cell Rep. Phys. Sci. 3 (2022), 100972.

[57] C.J. Peng, X.T. Wu, G. Zeng, Q.L. Zhu, In Situ Bismuth nanosheet assembly for highly selective electrocatalytic CO₂ reduction to formate, Chem. Asian J73 16 (2021) 1539–1544.

[58] S.N. Sun, L.Z. Dong, J.R. Li, J.W. Shi, J. Liu, Y.R. Wang, Q. Huang, Y.Q. Lan, Redox-active crystalline coordination catalyst for hybrid electrocatalytic methanol oxidation and CO₂ reduction, Angew. Chem. Int. Ed. 61 (2022).

[59] J. Tian, C. Cao, D.D. Ma, S.G. Han, Y. He, X.T. Wu, Q.L. Zhu, Killing two birds with one stone: selective oxidation of small organic molecule as anodic reaction to boost CO₂ electrolysis, Small Struct. 3 (2021) 2100134.

[60] Y.R. Wang, H.M. Ding, S.N. Sun, Jw Shi, Y.L. Yang, Q. Li, Y. Chen, S.L. Li, Y. Q. Lan, Light, Heat and electricity integrated energy conversion system: photothermal-assisted Co-electrolysis of CO₂ and methanol, Angew. Chem. Int. Ed. 61 (2022), e202212162.

[61] X. Wei, Y. Li, L. Chen, J. Shi, Formic acid electro-synthesis by concurrent cathodic CO₂ reduction and anodic CH₃OH oxidation, Angew. Chem. Int. Ed. 60 (2020) 3148–3155.

[62] D. Wu, J. Hao, Z. Song, X.Z. Fu, J.L. Luo, All roads lead to rome: an energy-saving integrated electrocatalytic CO₂ reduction system for concurrent value-added formate production, Chem. Eng. J. 412 (2021), 127893.

[63] C. Xiao, L. Cheng, Y. Wang, J. Liu, R. Chen, H. Jiang, Y. Li, C. Li, Low full-cell voltage driven high-current-density selective paired formate electrosynthesis, J. Mater. Chem. A. 10 (2022) 1329–1335.

[64] Y.L. Zhang, J. Lan, F. Xie, M. Peng, J.L. Liu, T.S. Chan, Y.W. Tan, Aligned InS nanorods for efficient electrocatalytic carbon dioxide reduction, ACS Appl. Mater. Interfaces 14 (2022) 25257–25266.

[65] L. Zhou, Z. Qu, L. Fu, Rational design of hollow nitrogen-doped carbon supported nickel nanoparticles for efficient electrocatalytic CO₂ reduction, J. Environ. Chem. Eng. 11 (2023), 109427.

[66] A. Saxena, S. Kapila, J.E. Medvedeva, M. Nath, Copper cobalt elenide as a bifunctional electrocatalyst for the selective reduction of CO₂ to carbon-rich products and alcohol oxidation, ACS Appl. Mater. Interfaces (2023) 14433–14446.

[67] M.S.E. Houache, R. Safari, U.O. Nwabara, T. Rafaïdeen, G.A. Botton, P.J.A. Kenis, S. Baranton, C. Coutanceau, E.A. Baranova, Selective electrooxidation of glycerol to formic acid over carbon supported Ni₁₋ₓMₓ (M=Bi, Pd, and Au) nanocatalysts and coelectrolysis of CO₂, ACS Appl. Energy Mater. 3 (2020) 8725–8738.

[68] Y. Pei, Z. Pi, H. Zhong, J. Cheng, F. Jin, Glycerol oxidation-assisted electrochemical CO₂ reduction for the dual production of formate, J. Mater. Chem. A 10 (2022) 1309–1319.

[69] G. Wang, J. Chen, K. Li, J. Huang, Y. Huang, Y. Liu, X. Hu, B. Zhao, L. Yi, T. W. Jones, Z. Wen, Cost-effective and durable electrocatalysts for Co-electrolysis of CO₂ conversion and glycerol upgrading, Nano Energy 92 (2022), 106751.

[70] J.R.C. Junqueira, D. Das, A. Cathrin Brix, S. Dieckhofer, J. Weidner, X. Wang, J. Shi, W. Schuhmann, Simultaneous anodic and cathodic formate production in a paired electrolyzer by CO₂ reduction and glycerol oxidation, ChemSusChem 16 (2023), e202202349.

[71] M.A. Bajada, S. Roy, J. Warnan, K. Abdiaziz, A. Wagner, M.M. Roessler, E. Reisner, A precious-metal-free hybrid electrolyzer for alcohol oxidation coupled to CO₂-to-syngas conversion, Angew. Chem. Int. Ed. 59 (2020) 15633–15641.

[72] J. Wang, X. Li, M. Wang, T. Zhang, X. Chai, J. Lu, T. Wang, Y. Zhao, D. Ma, Electrocatalytic valorization of poly(ethylene terephthalate) plastic and CO₂ for simultaneous production of formic acid, ACS Catal. 12 (2022) 6722–6728.

[73] E. Pérez-Gallent, S. Turk, R. Latsuzbaia, R. Bhardwaj, A. Anastasopol, F. Sastre-Calabuig, A.C. Garcia, E. Giling, E. Goetheer, Electroreduction of CO₂ to CO paired with 1,2-propanediol oxidation to lactic acid. toward an economically feasible system, Ind. Eng. Chem. Res. 58 (2019) 6195–6202.

[74] Y. Wang, S. Gonell, U.R. Mathiyazhagan, Y. Liu, D. Wang, A.J.M. Miller, T. J. Meyer, Simultaneous electrosynthesis of syngas and an aldehyde from CO₂ and an alcohol by molecular electrocatalysis, ACS Appl. Energy Mater. 2 (2018) 97–101.

[75] T. Li, Y. Cao, J. He, C.P. Berlinguette, Electrolytic CO₂ reduction in tandem with oxidative organic chemistry, ACS Cent. Sci. 3 (2017) 778–783.

[76] R. Li, K. Xiang, Z. Peng, Y. Zou, S. Wang, Recent advances on electrolysis for simultaneous generation of valuable chemicals at both anode and cathode, Adv. Energy Mater. 11 (2021) 2102292.

[77] S. Choi, M. Balamurugan, K.G. Lee, K.H. Cho, S. Park, H. Seo, K.T. Nam, Mechanistic investigation of biomass oxidation using nickel oxide nanoparticles in a CO₂-saturated electrolyte for paired electrolysis, J. Phys. Chem. Lett. 11 (2020) 2941–2948.

[78] J. Bi, Q. Zhu, W. Guo, P. Li, S. Jia, J. Liu, J. Ma, J. Zhang, Z. Liu, B. Han, Simultaneous CO₂ reduction and 5-hydroxymethylfurfural oxidation to value-added products by electrocatalysis, ACS Sustain. Chem. Eng. 10 (2022) 8043–8050.

[79] Z.W. Yang, J.M. Chen, L.Q. Qiu, W.J. Xie, L.N. He, Solar energy-driven electrolysis with molecular catalysts for the reduction of carbon dioxide coupled with the oxidation of 5-hydroxymethylfurfural, Catal. Sci. Technol. 12 (2022) 5495–5500.

[80] R. Lin, Energy efficient electrochemical system for combined carbon dioxide reduction and HMF oxidation, Department of Chemical Engineering McGill University, Montreal (2022).

[81] Z.W. Yang, J.M. Chen, Z.L. Liang, W.J. Xie, B. Zhao, L.N. He, Anodic product-derived Bi-MOF as pre-catalyst for cathodic CO₂ reduction: a novel strategy for paired electrolysis, ChemCatChem 15 (2022), e202201321.

[82] H. Liu, Y. Su, S. Kuang, E.J.M. Hensen, S. Zhang, X. Ma, Highly efficient CO₂ electrolysis within a wide operation window using octahedral tin oxide single crystals, J. Mater. Chem. A 9 (2021) 7848–7856.

[83] J.H. Guo, W.Y. Sun, Integrating nickel-nitrogen doped carbon catalyzed CO₂ electroreduction with chlor-alkali process for CO, Cl₂ and KHCO₃ production with enhanced techno-economics, Appl. Catal. B: Environ. 275 (2020) 119154.

[84] F. Quan, G. Zhan, H. Shang, Y. Huang, F. Jia, L. Zhang, Z. Ai, Highly efficient electrochemical conversion of CO₂ and NaCl to CO and NaClO, Green. Chem. 21 (2019) 3256–3262.

[85] X. Tan, C. Yu, X. Song, C. Zhao, S. Cui, H. Xu, J. Chang, W. Guo, Z. Wang, Y. Xie, J. Qiu, Toward an understanding of the enhanced CO₂ electroreduction in NaCl electrolyte over CoPc molecule-implanted graphitic carbon nitride catalyst, Adv. Energy Mater. 11 (2021) 2100075.

[86] C. Kang, Y. Li, Y. Xu, C. Ding, H. Chen, J. Zeng, Y. Li, C. Li, J. He, Coupling CO₂-to-ethylene reduction with the chlor-alkaline process in seawater through in situ-formed Cu catalysts, J. Phys. Chem. Lett. 14 (2023) 2983–2989.

[87] Z. Chen, K. Mou, X. Wang, L. Liu, Nitrogen-doped graphene quantum dots enhance the activity of Bi₂O₃ nanosheets for electrochemical reduction of CO₂ in a wide negative potential region, Angew. Chem. Int. Ed. 57 (2018) 12790–12794.

[88] B. Zhao, J. Liu, C. Xu, R. Feng, P. Sui, L. Wang, J. Zhang, J.L. Luo, X.Z. Fu, Hollow NiSe nanocrystals heterogenized with carbon nanotubes for efficient electrocatalytic methanol upgrading to boost hydrogen co-production, Adv. Funct. Mater. 31 (2020) 2008812.

[89] J. Hao, J. Liu, D. Wu, M. Chen, Y. Liang, Q. Wang, L. Wang, X.Z. Fu, J.L. Luo, In situ facile fabrication of Ni(OH)₂ nanosheet arrays for electrocatalytic co-production of formate and hydrogen from methanol in alkaline solution, Appl. Catal. B: Environ. 281 (2021), 119510.

[90] B. Zhao, J. Liu, X. Wang, C. Xu, P. Sui, R. Feng, L. Wang, J. Zhang, J.L. Luo, X. Z. Fu, CO₂-emission-free electrocatalytic CH₃OH selective upgrading with high productivity at large current densities for energy saved hydrogen co-generation, Nano Energy 80 (2021), 105530.

[91] W. Chen, C. Xie, Y. Wang, Y. Zou, C.L. Dong, Y.C. Huang, Z. Xiao, Z. Wei, S. Du, C. Chen, B. Zhou, J. Ma, S. Wang, Activity origins and design principles of nickel-based catalysts for nucleophile electrooxidation, Chem 6 (2020) 2974–2993.

[92] R.B. Song, W. Zhu, J. Fu, Y. Chen, L. Liu, J.R. Zhang, Y. Lin, J.J. Zhu, Electrode materials engineering in electrocatalytic CO₂ reduction: energy input and conversion efficiency, Adv. Mater. 32 (2019) e1903796.

[93] J. Hong, C. Xu, B. Deng, Y. Gao, X. Zhu, X. Zhang, Y. Zhang, Photothermal chemistry based on solar energy: from synergistic effects to practical applications, Adv. Sci. 9 (2022) 2103926.

[94] D. Li, X. Lang, Y. Guo, Y. Wang, Y. Wang, H. Shi, S. Wu, W. Wang, Q.H. Yang, A photo-assisted electrocatalyst coupled with superoxide suppression for high performance Li-O₂ batteries, Nano Energy 85 (2021), 105966.

[95] H. Huang, B. Weng, H. Zhang, F. Lai, J. Long, J. Hofkens, R.E. Douthwaite, J. A. Steele, M.B.J. Roeffaers, Solar-to-chemical fuel conversion via metal halide perovskite solar-driven electrocatalysis, J. Phys. Chem. Lett. 13 (2022) 25–41.

[96] N. Han, P. Ding, L. He, Y. Li, Y. Li, Promises of main group metal–based nanostructured materials for electrochemical CO₂ reduction to formate, Adv. Energy Mater. 10 (2019) 1902338.

[97] S. Wang, T. Kou, S.E. Baker, E.B. Duoss, Y. Li, Electrochemical reduction of CO₂ to alcohols: current understanding, progress, and challenges, Adv. Energy Sustain. Res. 3 (2021) 2100131.

[98] E.W. Lees, B.A.W. Mowbray, F.G.L. Parlane, C.P. Berlinguette, Gas diffusion electrodes and membranes for CO₂ reduction electrolysers, Nat. Rev. Mater. 7 (2021) 55–64.

[99] Á. Vass, B. Endrődi, C. Janáky, Coupling electrochemical carbon dioxide conversion with value-added anode processes: an emerging paradigm, Curr. Opin. Electrochem. 25 (2021), 100621.

[100] Y. Pan, X. Li, D. Su, Understanding the structural dynamics of electrocatalysts via liquid cell transmission electron microscopy, Curr. Opin. Electrochem. 33 (2022), 100936.

[101] L. An, F. Yang, C. Fu, X. Cai, S. Shen, G. Xia, J. Li, Y. Du, L. Luo, J. Zhang, A functionally stable RuMn electrocatalyst for oxygen evolution reaction in acid, Adv. Funct. Mater. 32 (2022) 2200131.

[102] Y.J. Wu, J. Yang, T.X. Tu, W.Q. Li, P.F. Zhang, Y. Zhou, J.F. Li, J.T. Li, S.G. Sun, Evolution of cationic vacancy defects: a motif for surface restructuration of OER precatalyst, Angew. Chem. Int. Ed. 60 (2021) 26829–26836.

[103] F. Altaf, R. Gill, R. Batool, M. Drexler, F. Alamgir, G. Abbas, K. Jacob, Proton conductivity and methanol permeability study of polymer electrolyte membranes with range of functionalized clay content for fuel cell application, Eur. Polym. J. 110 (2019) 155–167.

[104] L.T. Yogarathinam, J. Jaafar, A.F. Ismail, P.S. Goh, M.H. Bin Mohamed, M. F. Radzi Hanifah, A. Gangasalam, J. Peter, Polyaniline decorated graphene oxide on sulfonated poly(ether ether ketone) membrane for direct methanol fuel cells application, Polym. Adv. Technol. 33 (2021) 66–80.

[105] N.A. Ivanova, D.D. Spasov, R.M. Mensharapov, E.V. Kukueva, A.A. Zasypkina, V. N. Fateev, S.A. Grigoriev, Efficient and stable subzero operation of a PEM fuel cell with a composite anode using hydrogen-methanol composition during freeze/thaw cycles, Int. J. Hydrog. Energy 48 (2023) 11410–11420.

[106] Z. Zhang, E.W. Lees, S. Ren, B.A.W. Mowbray, A. Huang, C.P. Berlinguette, Conversion of reactive carbon solutions into CO at low voltage and high carbon efficiency, ACS Cent. Sci. 8 (2022) 749–755.

[107] J. Zhang, W. Luo, A. Züttel, Crossover of liquid products from electrochemical CO₂ reduction through gas diffusion electrode and anion exchange membrane, J. Catal. 385 (2020) 140–145.

[108] Y.C. Li, Z. Yan, J. Hitt, R. Wycisk, P.N. Pintauro, T.E. Mallouk, Bipolar membranes inhibit product crossover in CO₂ electrolysis cells, Adv. Sustain. Syst. 2 (2018) 1700187.

[109] P.K. Giesbrecht, M.S. Freund, Recent advances in bipolar membrane design and applications, Chem. Mater. 32 (2020) 8060–8090.

[110] H. Luo, J. Barrio, N. Sunny, A. Li, L. Steier, N. Shah, I.E.L. Stephens, M.M. Titirici, Progress and perspectives in photo- and electrochemical-oxidation of biomass for sustainable chemicals and hydrogen production, Adv. Energy Mater. 11 (2021) 2101180.

[111] A. Tursi, A review on biomass: importance, chemistry, classification, and conversion, Biofuel Res. J. 6 (2019) 962–979.

[112] Y. Meng, S. Yang, H. Li, Electro- and photocatalytic oxidative upgrading of bio-based 5-hydroxymethylfurfural, ChemSusChem 15 (2022), e202102581.

[113] S. Kunnikuruvan, N.N. Nair, Mechanistic insights into the brønsted acid-catalyzed dehydration of β-d-glucose to 5-hydroxymethylfurfural under ambient and subcritical conditions, ACS Catal. 9 (2019) 7250–7263.

[114] Y. Yang, T. Mu, Electrochemical oxidation of biomass derived 5-hydroxymethyl-furfural (HMF): pathway, mechanism, catalysts and coupling reactions, Green. Chem. 23 (2021) 4228–4254.

[115] X. Fu, Y. Hu, Y. Zhang, Y. Zhang, D. Tang, L. Zhu, C. Hu, Solvent effects on degradative condensation side reactions of fructose in its initial conversion to 5-hydroxymethylfurfural, ChemSusChem 13 (2020) 438.

[116] C. Xu, E. Paone, D. Rodriguez-Padron, R. Luque, F. Mauriello, Recent catalytic routes for the preparation and the upgrading of biomass derived furfural and 5-hydroxymethylfurfural, Chem. Soc. Rev. 49 (2020) 4273–4306.

[117] H. Zhang, J.H. Clark, T. Geng, H. Zhang, F. Cao, A carbon catalyst Co-doped with P and N for efficient and selective oxidation of 5–hydroxymethylfurfural into 2,5–diformylfuran, ChemSusChem 14 (2020) 456–466.

[118] E. Hayashi, Y. Yamaguchi, K. Kamata, N. Tsunoda, Y. Kumagai, F. Oba, M. Hara, Effect of MnO₂ crystal structure on aerobic oxidation of 5-hydroxymethylfurfural to 2,5-furandicarboxylic acid, J. Am. Chem. Soc. 141 (2019) 890–900.

[119] S. Yang, Y. Guo, Y. Zhao, L. Zhang, H. Shen, J. Wang, J. Li, C. Wu, W. Wang, Y. Cao, S. Zhuo, Q. Zhang, H. Zhang, Construction of synergistic Ni₃S₂-MoS₂ nanoheterojunctions on Ni foam as bifunctional electrocatalyst for hydrogen evolution integrated with biomass valorization, Small 18 (2022), e2201306.

[120] M. Park, M. Gu, B.S. Kim, Tailorable electrocatalytic 5-hydroxymethylfurfural oxidation and H₂ production: architecture-performance relationship in bifunctional multilayer electrodes, ACS Nano 14 (2020) 6812–6822.

[121] Y. Zhao, M. Cai, J. Xian, Y. Sun, G. Li, Recent advances in the electrocatalytic synthesis of 2,5-furandicarboxylic acid from 5-(hydroxymethyl) furfural, J. Mater. Chem. A. 9 (2021) 20164–20183.

[122] C.T. Dinh, T. Burdyny, M.G. Kibria, A. Seifitokaldani, C.M. Gabardo, F.P. Gd Arquer, A. Kiani, J.P. Edwards, P.D. Luna, O.S. Bushuyev, C. Zou, R. Quintero-Bermudez, Y. Pang, D. Sinton, E.H. Sargent, CO_2 electroreduction to ethylene via hydroxide-mediated copper catalysis at an abrupt interface, Science 360 (2018) 783–787.

[123] M.T. Bender, X. Yuan, M.K. Goetz, K.S. Choi, Electrochemical hydrogenation, hydrogenolysis, and dehydrogenation for reductive and oxidative biomass upgrading using 5-hydroxymethylfurfural as a model system, ACS Catal. 12 (2022) 12349–12368.

[124] J. Xu, G. Zhong, M. Li, D. Zhao, Y. Sun, X. Hu, J. Sun, X. Li, W. Zhu, M. Li, Z. Zhang, Y. Zhang, L. Zhao, C. Zheng, X. Sun, Review on electrochemical carbon dioxide capture and transformation with bipolar membranes, Chin. Chem. Lett. 34 (2023).

[125] C.M. Gabardo, C.P. O'Brien, J.P. Edwards, C. McCallum, Y. Xu, C.T. Dinh, J. Li, E. H. Sargent, D. Sinton, Continuous carbon dioxide electroreduction to concentrated multi-carbon products using a membrane electrode assembly, Joule 3 (2019) 2777–2791.

[126] J.C. Wu, L.T. Xu, Y.Y. Li, C.L. Dong, Y.X. Lu, T.T.T. Nga, Z.J. Kong, S. Li, Y.Q. Zou, S.Y. Wang, Anodic cross-coupling of biomass platform chemicals to sustainable biojet fuel precursors, J. Am. Chem. Soc. 144 (2022) 23649–23656.

[127] I.A. Moreno-Hernandez, B.S. Brunschwig, N.S. Lewis, Crystalline nickel, cobalt, and manganese antimonates as electrocatalysts for the chlorine evolution reaction, Energy Environ. Sci. 12 (2019) 1241–1248.

[128] K.S. Exner, Controlling stability and selectivity in the competing chlorine and oxygen evolution reaction over transition metal oxide electrodes, ChemElectroChem 6 (2019) 3401–3409.

[129] I.A. Digdaya, I. Sullivan, M. Lin, L. Han, W.H. Cheng, H.A. Atwater, C. Xiang, A direct coupled electrochemical system for capture and conversion of CO_2 from oceanwater, Nat. Commun. 11 (2020) 4412.

[130] W. Choi, M. Kim, Bj Kim, Y. Park, D.S. Han, M.R. Hoffmann, H. Park, Electrocatalytic arsenite oxidation in bicarbonate solutions combined with CO_2 reduction to formate, Appl. Catal. B: Environ. 265 (2020), 118607.

[131] A. Chen, B.L. Lin, A simple framework for quantifying electrochemical CO_2 fixation, Joule 2 (2018) 594–606.

[132] B. Pratap, S. Kumar, S. Nand, I. Azad, R.N. Bharagava, L.F. Romanholo Ferreira, V. Dutta, Wastewater generation and treatment by various eco-friendly technologies: Possible health hazards and further reuse for environmental safety, Chemosphere 313 (2023), 137547.

[133] J. Zhang, H. Wang, Y. Shao, G.H. Liu, L. Qi, W. Dang, J. Yuan, Y. Li, Z. Xia, Analysis on common problems of the wastewater treatment industry in urban China, Chemosphere 291 (2022), 132875.

[134] Q. Wang, C. Zhu, C. Wu, H. Yu, Direct synthesis of bismuth nanosheets on a gas diffusion layer as a high-performance cathode for a coupled electrochemical system capable of electroreduction of CO_2 to formate with simultaneous degradation of organic pollutants, Electrochim. Acta 319 (2019) 138–147.

[135] S. Sabatino, A. Galia, G. Saracco, O. Scialdone, Development of an electrochemical process for the simultaneous treatment of wastewater and the conversion of carbon dioxide to higher value products, Chemelectrochem 4 (2017) 150–159.

[136] M. Choi, J.W. Kim, S. Chung, Y. Lee, S. Bong, J. Lee, Syngas production for fischer-tropsch process via co-electrolytic processes of CO_2 reduction and NH_3 oxidation, Chem. Eng. J. 430 (2022) 132563.

[137] Q. Wang, W. Wang, C. Zhu, C. Wu, H. Yu, A novel strategy to achieve simultaneous efficient formate production and p-nitrophenol removal in a co-electrolysis system of CO_2 and p-nitrophenol, J. CO_2 Util. 47 (2021) 101497.

[138] M. Zhu, L. Zhang, S. Liu, D. Wang, Y. Qin, Y. Chen, W. Dai, Y. Wang, Q. Xing, J. Zou, Degradation of 4-nitrophenol by electrocatalysis and advanced oxidation processes using $Co_3O_4@C$ anode coupled with simultaneous CO_2 reduction via SnO_2/CC cathode, Chin. Chem. Lett. 31 (2020) 1961–1965.

[139] G. Bharath, K. Rambabu, C. Aubry, M. Abu Haija, A.K. Nadda, N. Ponpandian, F. Banat, Self-assembled Co_3O_4 nanospheres on N-doped reduced graphene oxide (Co_3O_4/N-RGO) bifunctional electrocatalysts for cathodic reduction of CO_2 and anodic oxidation of organic pollutants, ACS Appl. Energy Mater. 4 (2021) 11408–11418.

[140] Z. Li, Q. Zeng, Z. Ye, W. Zheng, X. Sang, C.L. Dong, B. Yang, S. Pardiwala, J. Lu, L. Lei, G. Wu, Y. Hou, An integrated bioelectrochemical system coupled CO_2 electroreduction device based on atomically dispersed iron electrocatalysts, Nano Energy 87 (2021), 106187.

[141] Y. Kong, L. Wang, H. Jiang, F. Li, T. Zhao, M. Zhuo, Q. Chen, M. Mao, Y. Xu, Design of counter oxidation vs. CO_2 electroreduction for efficient formate production on a tin cathode, J. Electroanal. Chem. 847 (2019), 113264.

[142] Y. Pei, C. Wang, H. Zhong, F. Jin, Concurrent electrolysis under pressured CO_2 for simultaneous CO_2 reduction and hazardous SO_2 removal, ACS Sustain. Chem. Eng. 10 (2022) 12670–12678.

[143] W. Ma, H. Wang, W. Yu, X. Wang, Z. Xu, X. Zong, C. Li, Achieving simultaneous CO_2 and H_2S conversion via a coupled solar-driven electrochemical approach on non-precious-metal catalysts, Angew. Chem. Int. Ed. 57 (2018) 3473–3477.

[144] B. Zhang, J. Bai, Y. Zhang, C. Zhou, P. Wang, L. Zha, J. Li, A. Simchi, B. Zhou, High yield of CO and synchronous S recovery from the conversion of CO_2 and H_2S in natural gas based on a novel electrochemical reactor, Environ. Sci. Technol. 55 (2021) 14854–14862.

[145] M. Li, T. Wang, W. Zhao, S. Wang, Y. Zou, A pair-electrosynthesis for formate at ultra-low voltage via coupling of CO_2 reduction and formaldehyde oxidation, Nano-Micro Lett. 14 (2022) 211.

[146] Y. Cao, X. He, N. Wang, H.R. Li, L.N. He, Photochemical and electrochemical carbon dioxide utilization with organic compounds, Chin. J. Chem. 36 (2018) 644–659.

[147] H.S. Pillai, H. Xin, New insights into electrochemical ammonia oxidation on Pt (100) from first principles, Ind. Eng. Chem. Res. 58 (2019) 10819–10828.

[148] A.Y. Zhang, Y.Y. He, Y.P. Chen, J.W. Feng, N.H. Huang, F. Lian, Degradation of organic pollutants by Co_3O_4-mediated peroxymonosulfate oxidation: Roles of high-energy {0 0 1}9-exposed TiO_2 support, Chem. Eng. J. 334 (2018) 1430–1439.

[149] Y. Jiang, X.P. Zhu, X. Xing, Electrochemical oxidation of phenolic compounds at boron-doped diamond anodes: structure-reactivity relationships, J. Phys. Chem. A 121 (2017) 4326–4333.

[150] P.J. Espinoza-Montero, P. Alulema-Pullupaxi, B.A. Frontana-Uribe, C.E. Barrera-Diaz, Electrochemical production of hydrogen peroxide on boron-doped diamond (BDD) electrode, Curr. Opin. Solid. St. M. 26 (2022), 100988.

[151] S. Kondaveeti, E. Kang, H. Liu, B. Min, Continuous autotrophic denitrification process for treating ammonium-rich leachate wastewater in bioelectrochemical denitrification system (BEDS), Bioelectrochemistry 130 (2019), 107340.

[152] Vandana, M. Priyadarshanee, U. Mahto, S. Das, Mechanism of toxicity and adverse health effects of environmental pollutants, Microb. Biodegrad. Biorem. (2022) 33–53.

[153] C. Gao, X. Feng, L. Yi, X. Wu, R. Zheng, G. Zhang, Y. Li, Peroxymonosulfate activation based on $Co_9S_8@N-C$: a new strategy for highly efficient hydrogen production and synchronous formaldehyde removal in wastewater, J. Mater. Sci. Technol. 127 (2022) 256–267.

[154] Y. Liang, Y. Zhou, Y. Shi, C. Liu, B. Zhang, Unveiling in situ evolved In/In_2O_3-heterostructure as the active phase of In_2O_3 toward efficient electroreduction of CO_2 to formate, Sci. Bull. 65 (2020) 1547–1554.

[155] Z.H. Zhu, Z.L. Liang, S.L. Hou, Y. Xie, Y. Ma, Y. Zhang, B. Zhao, Efficient CO_2 electroreduction coupled with semi-dehydrogenation of tetrahydroisoquinoline by MOFs modified electrodes, J. Energy Chem. 63 (2021) 328–335.

[156] X. Cao, Y. Wang, D. Tan, B. Wulan, J. Ma, W. Guo, J. Zhang, Stepwise dispersion of nickel species for efficient coupling of electrocatalytic redox reactions, Chem. Eng. J. (2023), 140062.

[157] D.D. Ma, S.G. Han, C. Cao, W. Wei, X. Li, B. Chen, X.T. Wu, Q.L. Zhu, Bifunctional single-molecular heterojunction enables completely selective CO_2-to-CO conversion integrated with oxidative 3D nano-polymerization, Energy Environ. Sci. 14 (2021) 1544–1552.

[158] S. Zhong, Z. Cao, X. Yang, S.M. Kozlov, K.W. Huang, V. Tung, L. Cavallo, L.J. Li, Y. Han, Electrochemical conversion of CO_2 to 2-bromoethanol in a membraneless cell, ACS Energy Lett. 4 (2019) 600–605.

[159] X. Li, S.G. Han, W. Wu, K. Zhang, B. Chen, S.H. Zhou, D.D. Ma, W. Wei, X.T. Wu, R. Zou, Q.L. Zhu, Convergent paired electrosynthesis of dimethyl carbonate from carbon dioxide enabled by designing the superstructure of axial oxygen coordinated nickel single-atom catalysts, Energy Environ. Sci. 16 (2023) 502–512.